Journal of Materials Chemistry C

ROYAL SOCIETY OF CHEMISTRY

REVIEW

View Article Online
View Journal | View Issue

Cite this: J. Mater. Chem. C, 2020, 8, 15956

Metals in polymers: hybridization enables new functions

Zichao Wei, [a] Hanyi Duan,[b] Gengsheng Weng *[c] and Jie He *[ab]

Adding metals into synthetic polymers is of broad interest to design multifunctional materials, particularly harnessing unique properties and functionalities not found in pure organic polymers. Other than simple emergence of the two, such hybridization often enables synergies to amplify the existing properties and/or create new properties not existing in either component. In this review, we highlight recent examples of metal/polymer hybrids based on either well-defined or ill-defined metal–ligand (M–L) coordination to design multifunctional materials. This review describes how in the hybridization of metal ions and polymers they complement each other synergistically in terms of their optical, mechanical and catalytic functionalities. Synthetic polymers once bound to metals enable stimuli-responsive properties of the metals and control over the luminescence of the metals in response to a change in the environment. As the second coordination sphere, synthetic polymers also enhance the reactivity of metal sites as a means to design bioinspired artificial enzymes. Additionally, the impact of the M–L coordination on the dynamic properties of polymers is summarized in the context of self-healable and tough materials built on the reversible network of interchangeable M–L coordination.

Received 10th August 2020,
Accepted 6th October 2020

DOI: 10.1039/d0tc03810e

rsc.li/materials-c

1. Introduction

Traditionally, design of functional polymers relies on their chemical identity. Modifying polymers with specific chemical moieties endows them with the desired functionality. Taking the phase transition as an example, water-soluble polyacrylamide becomes thermoresponsive when simply replacing one H atom of the amide group with an isopropyl moiety, known as poly(N-isopropylacrylamide) (PNIPAM).[1] PNIPAM shows a lower critical solution temperature (LCST, around 32 1C) and a

[a] Department of Chemistry, Institute of Materials Science, University of Connecticut, Storrs, Connecticut 06269, USA. E-mail: jie.he@uconn.edu
[b] Polymer Program, Institute of Materials Science, University of Connecticut, Storrs, Connecticut 06269, USA
[c] State Key Laboratory Base of Novel Functional Materials and Preparation Science, Ningbo Key Laboratory of Specialty Polymers, School of Materials Science and Chemical Engineering, Ningbo University, Ningbo, 315211, China. E-mail: wenggengsheng@nbu.edu.cn

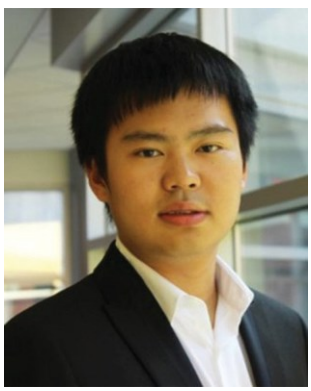

Zichao Wei

Zichao Wei received his Bachelor's degree in Chemical Engineering from Shenyang University of Chemical Technology. He obtained his Master's degree in Chemical Engineering from University of Connecticut in 2017. Currently he is a PhD student at the Department of Chemistry at the University of Connecticut under the supervision of Prof. Jie He. His research focus is on the design of new polymer/metal hybrids and their applications in elastomers and catalysis.

Hanyi Duan

Hanyi Duan received his MS degree in Polymer Chemistry from Zhejiang University in 2018, where he conducted research on stimuli-responsive polymers under the supervision of Prof. Xinghong Zhang and Binyang Du. Currently he is a PhD student at the polymer program at the Institute of Materials Science, University of Connecticut, under the supervision of Profs. Jie He and Yao Lin. His research interests include the synthesis and applications of metallopolymers, CO_2 reduction and self-assembly of plasmonic nanoparticles.

reversible phase transition in water. Not surprisingly, the LCST of poly(N-alkyl substituted acrylamide) is highly tunable by varying such chemical identity, e.g., the alkyl groups or copolymerization with other monomers, as reported previously.[2,3] In those systems, a single functionality can be added-in or varied through synthetic tools similar to that of thermoresponsiveness. Those materials with a single functionality, however, unlikely meet the rising demands of mankind to design more efficient and sophisticated devices. Design of new materials integrated with different functions is of essential importance in response to such demands. Yet, there are profound challenges to design those multifunctional materials in terms of (i) solving the compatibility of various functions;[4] and (ii) evolving new functions not existing in organic polymers. For example, common organic polymers that usually do not have single or unpaired electrons are not useful as a contrast agent in magnetic resonance imaging (MRI). One way to bring new functionalities to polymers is hybridization, which has been of long practice in materials chemistry and engineering. An obvious case is to solve the thermal and electric conductivity of organic polymers through hybridization with carbon and metallic nanomaterials.

Metals, broadly defined as metal ions, clusters and nanoparticles, have many unique properties and thus corresponding functionalities, e.g., luminescence,[5] magnetism,[6] plasmon resonance[7] and catalysis.[8] When binding or simply mixing metals with organic polymers, those properties can be added up in the resultant hybrids. Gadolinium (Gd^{3+}) containing polymers as an example have strong relaxivity and low toxicity for MRI examination.[9] Hybridization of those metal species with organic polymers not only simply offers merged properties of the two different components but also enables new synergies, i.e., amplifying the existing functionalities or creating ensemble functionalities not existing in the two components. Those, again, have been of long practice in the design of metal/polymer hybrids. Binding late transition metals with organic or polymeric chromophores can populate the triplet states, which are of great interest in electroluminescent materials for light-emitting diodes and photovoltaics.[10] Noble metal nanoparticles assembled with polymer ligands show the strong coupling of the plasmonic field, leading to new resonance peaks that cannot be found in either polymers or individual nanoparticles.[11–13] Such collective properties enable new functionalities of those hybrids in colorimetric sensing,[14] photocatalysis[15] and enhanced Raman scattering.[16] Coordinating catalytic inactive or less active metal cations with synthetic polymers can significantly improve their reactivity.[17] As such, the presence of metals in organic polymers shows great potential to drive the development of multifunctional materials.

Given the interdisciplinary nature, one of the key challenges in those metal/polymer hybrids is to understand their structure–function correlations. As mentioned in the broad definition of metals, hybridization of metals and polymers crosses size ranges from molecular and macromolecular to nanometer scales. There is a large body of work on multifunctional materials of metal/polymer hybrids that is not covered in this review, due to the limited knowledge of the authors. For example, nanoclusters of noble metals/polyoxometalates and various metal nanoparticles can bind with polymers as well to design new multifunctional materials. We refer the interested reader to some of the excellent reviews on those topics by Kumacheva,[18] Liu,[19] Nie[20] and Tao.[21] We will narrow our topics down to organic polymers incorporated with metal ions through metal–ligand (M–L) coordination as backbones or side chains. The focus of the current review is to highlight a few examples of metal/polymer hybrids based on either well-defined or ill-defined M–L coordination structures as multifunctional materials. The emphasis will be placed on how in hybridization of metals and polymers they complement each other synergistically to enable the functionalities of the resultant materials, that is, the uniqueness of each component to control the outcome of hybridization.

First of all, binding with metals varies the dynamics of polymer chains. As a typical example, metal cations that coordinate with a

Gengsheng Weng

Gengsheng Weng received his doctoral degree in Polymer Science and Engineering from Sichuan University in 2012. Since then, he has been working at the School of Materials Science and Chemical Engineering, Ningbo University, where he is currently an Associate Professor of polymer materials. In 2016–2017, he was a Visiting Professor at Prof. Jie He's group at the University of Connecticut. His research interests lie in responsive polymer elastomers, high-performance rubber materials, and hydrogels of polymer/metal hybrids.

Jie He

Jie He received his BS and MS degrees in Polymer Materials Science and Engineering from Sichuan University and his PhD in Chemistry from Universite de Sherbrooke in 2010. After working with Professor Zhihong Nie as a postdoctoral fellow at the University of Maryland, he joined the faculty of the University of Connecticut where he is currently an Associate Professor of Chemistry. His group focuses on the design of hybrid materials of polymers and inorganic materials (metal ions, clusters and nanoparticles) being capable of catalyzing the activation of H_2O, O_2 and CO_2 as inspired by nature.

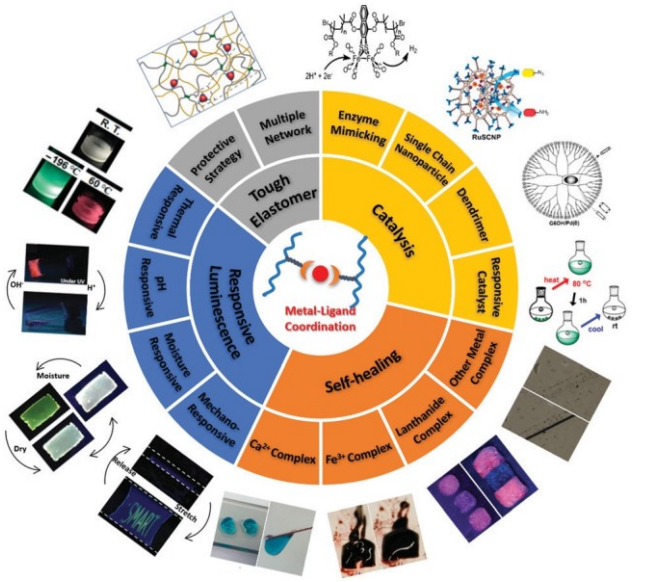

Scheme 1 Schematic summary of representative application areas derived from the polymeric metal–ligand interaction. (1) Blue regimes, responsive luminescence metal/polymer hybrids, figures reproduced from ref. 22, copyright 2015 American Chemical Society;[22] ref. 23, copyright 2018 Wiley VCH;[23] ref. 24 and 25, copyright 2019 Wiley VCH.[24,25] (2) Orange regime, self-healable metal/polymer hybrids, figures reproduced from ref. 26, copyright 2017 American Chemical Society;[26] ref. 27;[27] ref. 23, copyright 2018 Wiley VCH;[23] ref. 28, copyright 2019 Elsevier B.V.[28] (3) Yellow regime, catalysis of metal/polymer hybrids, figures reproduced from ref. 29, copyright 2015 American Chemical Society;[29] ref. 30, copyright 2001 American Chemical Society;[30] ref. 31, copyright 2020 American Chemical Society;[31] ref. 32, copyright 2019 Wiley VCH.[32] (4) Grey regime, tough elastic metal/polymer hybrids, figure reproduced from ref. 24, copyright 2019 Wiley VCH.[24]

few ligands at one time can interact with a polymer intermolecularly to result in non-covalent cross-links. The network built on dynamic M–L interactions instantly exchanges, i.e., dissociates and reforms at the same time. With any mechanical rupture of those hybrids, such a non-covalent network can restructure to repair the damage through the dynamic exchange of M–L complexes, known as self-healable materials (Scheme 1). The healing efficiency is dependent on the M–L binding strength, the coordination number of metal sites and even the counter ions of the metals, as summarized in Section 3. The reversible M–L interactions also make it possible to dissipate the mechanical energy upon deformation, which largely improves the toughness of the polymers. Using M–L coordination together with a strong network formed by covalent cross-linking, one can design tough elastic materials highly resistant to mechanical failure, as discussed in Section 4. On the other hand, polymers show a great impact on, or determine in some cases, the functionalities of metals (Scheme 1). We review some recent advances in stimuli-responsive luminescent metal/polymer hybrids with a particular emphasis on emissive lanthanides. We highlight two design mechanisms based on coordination disruption and coordination competition to switch ON/OFF the emission of lanthanides in Section 2. At the end, we discuss the synergies of synthetic polymers with the catalytic activity of metal ions. The role of synthetic polymers, particularly the positive effect on the reactivity of metal sites, is spotlighted as a means to design bioinspired artificial enzymes. We would like to point out that many other functionalities of metal/polymer hybrids, such as electroluminescence,[33] antifouling,[34] and magnetism,[6] have not been included in the current review.

2. Responsive luminescence of metal/polymer hybrids

Changes in the luminescent properties of metal/polymer hybrids are among the most direct outcomes when hybridizing metals and polymers. Lanthanides, as an example, with interesting d–f excitation, enable intense and sharp metal-centered luminescence (including fluorescence and phosphorescence) to cover the entire range of the UV and visible spectra.[35,36] When incorporating with sensitizing ligands in the coordination sphere, the strong ''antenna effect'' shows enhancement in the emission of lanthanide metals.[37] The ''antenna effect'' refers to lanthanide complexes with light harvesting ligands which usually absorb light and have energy transfer to metal ions to enhance lanthanide-centered emission. Therefore, the disruption of M–L coordination, particularly the removal of antenna chromophores in the coordination sphere of lanthanides, will diminish their emission intensity. Given the dynamic nature of coordination, potential reversible luminescence switch ''ON/OFF'' can be designed in response to external stimuli, e.g., temperature, light, pH, electrical fields, ionic strength and mechanical forces, under which the coordination can dissociate and then reversibly reform. Alternatively, organic polymers with fluorophores also show intriguing responsiveness upon binding with metals. For example, when coordinating with late transition metals, the charge transfer from ligands to metals potentially leads to phosphorescence or fluorescence quenching in some cases.[38,39] Incorporating metals also enhances the charge carrier mobility and changes the photoconductivity of polymers.[40–43] The change in the polymer physical state likely has impacts on the luminescent properties of metals, and new reversible responsiveness of the luminescent properties of these hybrids could be enabled. Once coupled with the dynamic nature of M–L coordination, the mechanical strength of hybrid materials, e.g., sol–gel[44] or soft–tough transitions,[45] potentially shows a similar and coupled response with the luminescent properties.

In the case of lanthanide-containing hybrids, the luminescent properties of metals show strong dependence on the coordination. Reversible ON/OFF switching of the emission can be designed using two different methodologies. The first method is called coordination disruption. When coordinated with ligands having strong light absorption, the antenna effect will enhance the lanthanide emission through a ligand-to-metal energy transfer process. Any stimuli that disrupt the coordination between lanthanides and ligands can weaken the antenna effect and thus reduce the metal-centered luminescence. The second design is based on coordination competition. The O–H bond vibration can quench the fluorescence of lanthanides when it exists in the first coordination sphere.[46–48] With competitive binding of ligands like water

and alcohols, lanthanides favor binding with O atoms in those ligands, leading to the quenching of the lanthanide luminescence. Both methodologies are possible to use to design reversible switch ON/OFF of the emission of metals due to the dynamic nature of coordination.

2.1 Coordination disruption

One of the early examples from Rowan et al. demonstrated the responsive emission of lanthanides to couple with the sol–gel transition of supramolecular gels.[37,49] 2,6-Bis(benzimidazolyl)-pyridine (Mebip) as a tridentate ligand has strong absorption around 330 nm.[50] Capped with a poly(ethylene glycol) (PEG) oligomer (Fig. 1a), Mebip can coordinate a number of transition metals. Small early transition metal ions, e.g. Co^{2+} or Zn^{2+}, are able to bind with two Mebips in a twisted octahedron, while larger lanthanide ions can coordinate three Mebips. Upon coordination with mixed metals, like Zn^{2+}/Eu^{3+} pairs, organogels with strong red emission could be readily formed with the Eu–Mebip coordination as physical cross-linkers. Gelation resulted from crystallization of the globular particles generated by coordination supramolecules as revealed by X-ray diffraction.[51] Given the dynamic and reversible nature of M–L binding, one would expect

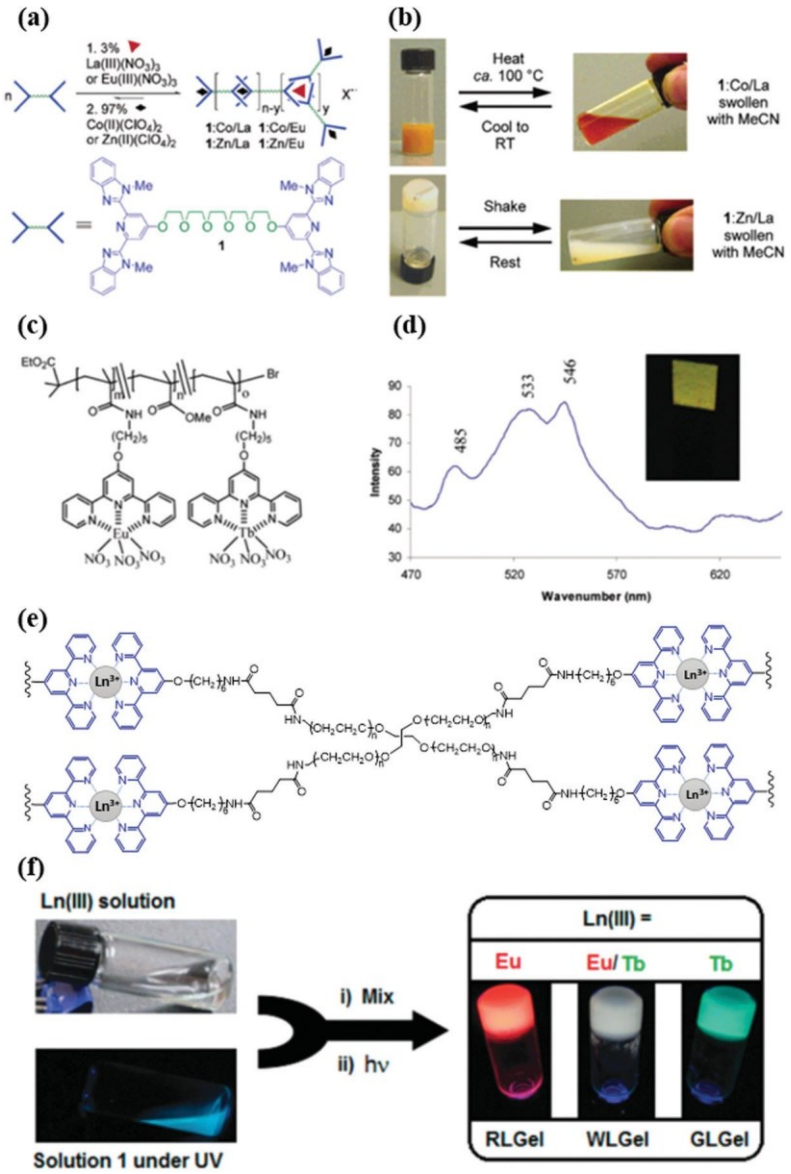

Fig. 1 (a) Schematic illustration of the formation of metal-containing supramolecular gels linked by lanthanides and other transition metal ions. (b) Thermo- and mechanoresponsive sol–gel transition of supramolecular gels. (c) Molecular structure of Eu^{3+}/Tb^{3+} containing PMMA with terpyridine pendants. (d) Photoluminescence spectrum of the solid film of Eu^{3+}/Tb^{3+} ions in PMMA as an "alloy" with an excitation wavelength of 350 nm. (e) Chemical structures of the four-arm terpyridine containing PEG and its coordination with metal ions. (f) Pictures of PEG metallogels showing the luminescence under UV light. The excitation wavelength is 365 nm. Figure (a and b) reproduced from ref. 37, copyright 2003 American Chemical Society;[37] figure (c and d) reproduced from ref. 52, copyright 2005 American Chemical Society;[52] figure (e and f) reproduced from ref. 22, copyright 2015 American Chemical Society.[22]

a reversible sol–gel transition of the organogels in response to various stimuli that disrupt the coordination, including temperatures, changes in pH and mechanical forces. For example, upon heating to ca. 100 1C or shaking, a clear sol–gel transition was seen as a result of the dissociation of Mebip–Ln coordination (Fig. 1b). The sol–gel transition was coupled with the luminescent properties of lanthanides, where no emission was seen in the sol state without Mebips in the first coordination sphere. By varying the M–L complexation with different stabilities, counterions of metal salts, and possible cores of the ligand-terminated monomers, a wide variety of stimuli-responsive supramolecular gels can be designed.[44]

Compared with supramolecular complexes, lanthanide complexes can be designed in polymer gels or elastomers with high elasticity, stiffness and toughness, while the luminescence of lanthanides as a probe can monitor the change in polymer networks.[24,45,53–57] Using telechelic copolymers of poly(ethylene-co-butylene) terminated with Mebip (M_w 4400 g mol^{-1}), Weder and coworkers prepared Eu^{3+}-containing elastomers with an intriguing mechanochemical response due to the dynamic properties of Mebip–Ln binding.[58] Under ultrasound sonication, the emission intensity of Eu^{3+} ions dropped by 20% as a result of the disruption of Mebip–Ln coordination. The red emission recovered within a few minutes once the sonication stopped. The recovery kinetics of luminescence appeared to be first order, much slower than that in small molecule complexes. As a comparison, polymers containing dipicolinic acid (dpa) did not dissociate under sonication. Mechanical force therefore provides a valuable non-invasive tool to control the dynamic binding of lanthanides in polymers to design smart materials capable of transducing forces into directly readable optical signals.

Sensitizing ligands can be grafted as the polymer side chains to coordinate metals. When coupled with two or more lanthanide metals in polymers, new stimuli-responsive luminescence can be expected due to the imposed steric impact from the macromolecular architectures. Using random copolymers of poly(methyl methacrylate) (PMMA) with terpyridine moieties, emissive lanthanide metals like Eu^{3+} and Tb^{3+} can be incorporated into polymer films (Fig. 1c).[52] Terpyridine has UV absorption around 290 nm[59] and it is a tridentate ligand for a variety of metals. Incorporating Eu^{3+} and Tb^{3+} into terpyridine-containing PMMA films would result in red and green emissive films, respectively. When stoichiometrically mixing Eu^{3+} and Tb^{3+} ions in the polymer at 1 : 1 (mol), the hybrid films showed a new emission peak at 533 nm that did not exist in individual Eu^{3+} and Tb^{3+}-containing films (Fig. 1d). As a coordination alloy, the film was yellow emissive (Fig. 1d). In contrast, when the two metals were mixed with the same polymer separately, the resultant films containing the two ions had green emission. The concurrent incorporation of Eu^{3+} and Tb^{3+} ions into the same polymer backbone resulted in an intimate spatial arrangement, possibly bridging bimetallic complexes through p–p stacking of terpyridine. This yellow-emissive film showed reversible thermochromism where orange emission was observed at 50 1C, while the yellow emission recovered at room temperature.

When balancing the emission of several lanthanides, e.g., Eu^{3+} (red), Tb^{3+} (green) and Dy^{3+} (blue), white emitting phosphors can be designed. Compared with other white-light-emitting dyes, lanthanide metal ions are mostly colorless, and therefore it is possible to design transparent white emitting polymers. In terpyridine-containing polymers, Tew and coworkers reported the facile production of true white-light emitting phosphors in solution or solid states.[60] The copolymers containing polystyrene (PS) and terpyridine can incorporate Eu^{3+}, Tb^{3+} and Dy^{3+} simultaneously at any given ratio to tune the emission color. A molar ratio of 1 : 1 : 1.8 (Eu^{3+} : Tb^{3+} : Dy^{3+}) gave a true white-light emitting film with CIE (International Commission on Illumination) coordinate values of (0.31, 0.33). White-light emitting phosphors can also be designed using two emitters, like a blue-emitting Dy^{3+}-chelated polymer and red-emitting Ru^{3+} complexes through coupled energy transfer from blue-emitting Dy^{3+} to the blue-absorbing Ru^{3+} complexes.[61] As the luminescence of lanthanides is stimuli-responsive, fluorochromic materials can therefore be designed when varying the emission intensity of lanthanides.[22,24,44,58,62–68]

The mixing of Eu^{3+} (red) and Tb^{3+} (green) ions in polymers can produce white emissive phosphors as well. Using a terpyridine end-capped four-arm PEG (4-Arm-PEG) (Fig. 1e), Holten-Andersen et al. developed hybrid organogels consisting of two lanthanide metals, i.e., Eu^{3+} and Tb^{3+}. The 4-Arm-PEG acted as a perfect physical cross-linker at a terpyridine:Ln molar ratio of 2 : 1, mol. The gels showed a tunable and stimuli-responsive luminescence color. Varying the molar ratio of Eu^{3+} and Tb^{3+} ions led to the formation of organogels with a broad spectrum of emission (Fig. 1f). At an Eu-to-Tb molar ratio of 4 : 96, a white-light emissive gel with a CIE color space of (0.30, 0.49) was obtained. The stimuli-responsive properties of those lanthanide-containing gels were explored under mechanical force, chemical vapor, temperature and pH.[22] For example, the gel-to-sol transition occurred when subjected to ultrasonication induced mechanical force. Under 5 min sonication, the gel broke down and the white emission changed to blueish as a result of Ln-terpyridine dissociation. Interestingly, the gels showed nontrivial green-white-red thermochromism under cryogenic conditions. When cycled from −196 to 60 1C, a reversible change in emission color from green to white and eventually to red was observed. The distinctive thermochromism change was caused by the intrinsic energy transfer from Tb^{3+} to Eu^{3+} at a higher temperature.

Coordination ligands can be incorporated on polymer backbones in the formation of coordination polymers[70] or metallopolymers.[6] Here, coordination polymers refer to inorganic polymers built on metals as linkers on the backbone while metallopolymers have organic polymer backbones coordinated with some metals ions. Using lanthanides in the backbone of copolymers, Weng's group demonstrated two methods to prepare elastic metallo-supramolecular films using 2,6-bis(1,2,3-triazol-4-yl)pyridine (BTP) to bind lanthanides. The first method was to use bispropylene-functionalized BTP, which reacted with di-thiol-ended polytetrahydrofuran (PTHF) via a photo-initiated thiol–ene reaction (Fig. 2a).[69] The second method was to incorporate bis-propanol as a chain extender to react with diisocyanate in polyurethane (Fig. 2b).[62] Both polymers could coordinate transition metals, like Eu^{3+}, Tb^{3+} and Zn^{2+}. The BTP ligands bound

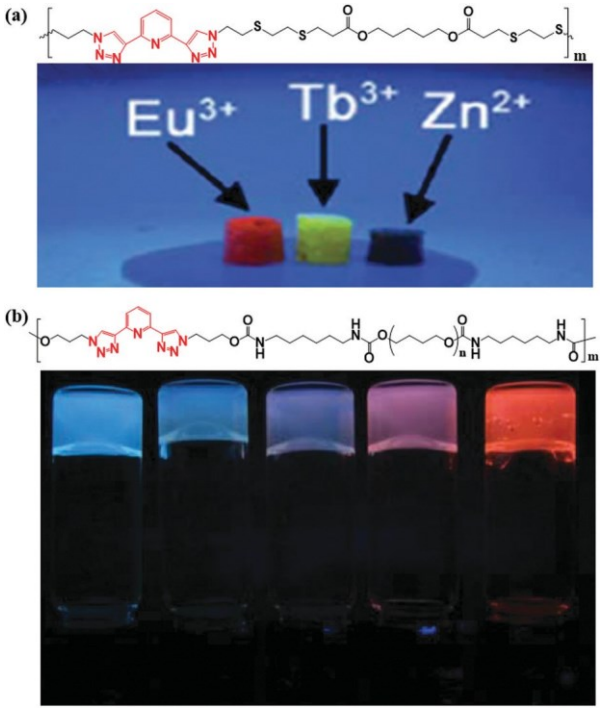

Fig. 2 (a) Fluorescence image of the three gels containing different metal ions (the Eu : Tb : Zn ratios from left to right are 100 : 0 : 0, 0 : 100 : 0 and 0 : 0 : 100) under UV light (254 nm). The structure of bisthiol functionalized polytetrahydrofurnan (PTHF) with multiple BTP is shown at the bottom. (b) Image of the gels with different amounts of Zn and Eu ions (from left to right Zn/Eu: 100/0, 75/25, 50/50, 25/75 and 0/100) under 365 nm UV light. The structure of polyurethane containing the BTP metal moiety is shown as an inset in this image. Figure (a) reproduced from ref. 69, copyright 2014 The Royal Society of Chemistry.[69] Figure (b) reproduced from ref. 62, copyright 2012 The Royal Society of Chemistry.[62]

with Eu^{3+} weakly and the coordination was more dynamic than that of Zn^{2+}. For polyurethane gels containing Eu^{3+} and Zn^{2+} ions, the dynamic properties of those gels were different. With 100% Zn^{2+} (100/0, Zn^{2+}:Eu^{3+}), the gel-to-sol transition occurred at 140 1C upon heating. The gel-to-sol transition temperature became lower, ca. 120 1C and 110 1C for the gels containing 75% and 100% Eu^{3+} with respect to Zn^{2+}, respectively. Such a thermo-responsive sol–gel transition was accompanied by emission quenching of Eu^{3+} where no emission was seen in the sol state. On cooling back to ambient temperature, gels were reformed along with the recovery of the Eu^{3+} emission.

When incorporating emissive lanthanides in fluorescent oligophenylenevinylene (OPV, Fig. 3a), Balamurugan's group designed carboxylic acid (as the ligand) functionalized p-conjugated polymer–Eu^{3+} ion complexes for thermosensitive luminescent switching in the solution and solid states.[66] When varying the length of oligo(ethylene glycol), the excitation and emission spectra of those OPV polymers were nearly identical with their maximum peaks at 350 nm and 610 nm, respectively. The quantum yields of those polymers were in the range of 0.13–0.27 in solution. When bound with Eu^{3+} ions, excitation energy transfer from p-conjugated OPVs to Eu^{3+} ions was evidenced from the emission quenching of polymers and subsequently produced sharp emission in the range of 570–720 nm from Eu^{3+} ions (Fig. 3b). Those OPVs therefore sensitized Eu^{3+} ions as ''antennae''. The luminescence intensity of Eu^{3+} ions was strongly impacted by temperature in both the solution and solid states. The emission intensity of Eu^{3+} ions slowly decreases with increasing temperature. Upon heating to 100 1C, the red emission from Eu^{3+} ions was completely shut down, as a result of the dissociation of the p-conjugated OPV–Eu^{3+} coordination at high temperatures (Fig. 3c). The thermosensitivity of those luminescent hybrids had a dependence on the polymer structures. With a longer length of oligo(ethylene glycol), higher breakdown temperatures at which the change in luminescence became active and higher luminescence contrasts were observed.

2.2 Coordination competition

It is challenging to have lanthanide based luminescent hydrogels with intense emission and high mechanical strength. One of the critical reasons is the hydration of lanthanide ions. Water can bind with emissive lanthanides in their first coordination sphere, and then the O–H vibration as an oscillator can quench the luminescence of lanthanides.[46] Weak binding motifs to lanthanides, like some monodentate or bidentate N ligands, can be disrupted by water. For example, there are numerous examples of using molecular Eu^{3+} complexes to pick up a trace amount of water from organic solvents as a means to detect water qualitatively since water quenches the emission of Eu^{3+}.[45,71–73] Water can even displace a strong 'tripod' ligand like tris(2-pyridylmethyl) amine.[74] Therefore only with some ligands can luminescent lanthanides be used under aqueous conditions.[75,76] In the presence of strong binding motifs in polymers, it is possible to directly have luminescent lanthanides in water.[77–79]

Our group designed Eu-containing polymer hydrogels that have fast self-healing and tunable fluorochromic properties in response to multiple stimuli.[23] We used a strong ligand iminodiacetate (IDA) as binding motifs to coordinate Eu^{3+} ions, which further acted as cross-linkers to prepare polymer hydrogels. IDA is known to have a large binding constant (K_b, the rate constant ratio of coordination on to off, $K_b = k_{on}/k_{off}$) to various metals,[80] while large lanthanide ions can coordinate with three to four IDA ligands simultaneously (Fig. 4a). Using copolymers of poly(N,N-dimethylacrylamide-co-3-iminodiacetate-2-hydroxypropylmethacrylate) ($P(DMA_{290}$-co-$IDHPMA_{96})$), the formation of Ln–IDA effectively excludes water from the coordination sphere of Eu^{3+} ions in the presence of excess IDA ligands in polymers. When adding Eu^{3+} ions to the polymer, a clear sol–gel transition was observed even at a low Eu content, e.g., a ratio Eu : IDA of 1/7, mol. The as-resultant Eu^{3+}-containing hydrogels showed typical red emission of Eu^{3+} complexes. The emission of Eu^{3+} ions was not strong compared with those antenna-type ligands. Since IDA is a tridentate ligand with deprotonated carboxylic acids and one tertiary amine, changes in pH can modulate the coordination strength of IDA with Eu^{3+}. Under acidic conditions, the protonation of the two acetates and the amine led to the dissociation of Eu–IDA. In the absence of IDA, the hydration also quenched the emission of Eu^{3+} ions. Therefore, those Eu-containing hydrogels underwent a reversible

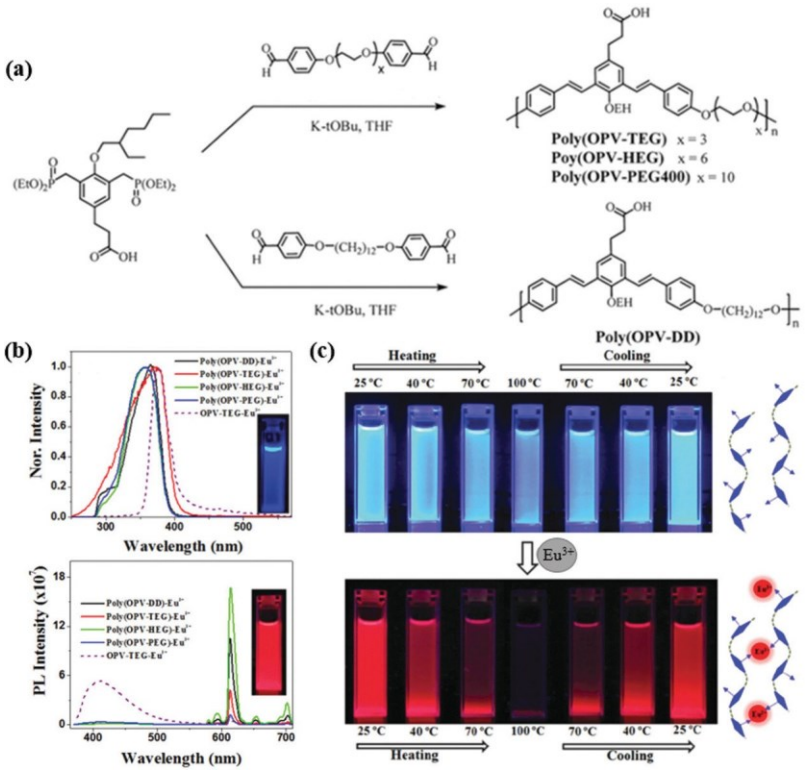

Fig. 3 (a) Synthesis of conjugated OPV polymers with binding sites. (b) Excitation (emission wavelength = 615 nm) (upper) and emission (lower) of the polymer and complexes in chlorobenzene. (c) Images of the polymer (upper) and polymer–Eu^{3+} complex (lower) in chlorobenzene at different temperatures. Figures reproduced from ref. 66, copyright 2013 The Royal Society of Chemistry.[66]

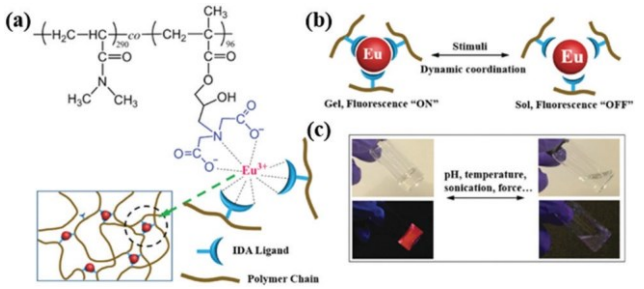

Fig. 4 (a) Chemical structure of IDA containing polymers and the cross-linking with Eu^{3+} ions. (b) Scheme showing the sol–gel transition and luminescence ON/OFF of Eu^{3+} containing polymers. (c) Digital pictures showing the sol–gel transition and fluorescence ON–OFF with external stimuli. Figures reproduced from ref. 23, copyright 2018 Wiley VCH.[23]

gel–sol transition along with switchable luminescence of Eu^{3+} ions in response to a change in pH as shown in Fig. 4. Other small transition metal ions, like Fe^{3+}, Zn^{2+} and Cu^{2+}, can be used as competitive ligands to weaken the binding of Eu–IDA. For smaller ions, e.g., Fe^{3+}, Zn^{2+} and Cu^{2+}, the binding pocket of IDA fits better with one ion. When adding smaller ions in those Eu-containing hydrogels, a similar sol–gel transition could be observed. For example, with a low concentration of Fe^{3+}, ~4 mM, the emission of Eu could be completely quenched. Similarly, heating, sonication and mechanical force could induce a gel-to-sol transition of Eu-containing hydrogels. These multistimuli-responsive fluorochromic hydrogels possibly can be used in conjugation with fluorophores that are not stimuli-responsive. A high contrast change of the emission color therefore can be gained for those hybrid materials.[24,64,81] For example, when coupled with green emissive fluorescein, Eu-containing polymers can vary their emission color from white to green where the red emission of Eu^{3+} is switchable in response to stimuli.[24] Such stimuli-responsiveness illustrates a new method to make smart optical materials, particularly for applications in biological sensors where multistimuli responsiveness is required.[35,82–89]

Control of lanthanide luminescence can be coupled with other luminescent materials, like carbon dots (CDs).[64] When varying the ratio of RGB emitters, one can fabricate white-light emitting phosphors as aforementioned. In addition, Holten–Andersen's group designed mechanochromic polymer films by the physical separation of fluorophores in a layered film.[25] Using CDs and lanthanide ions as the emitting species in the top and bottom layers of polymer films, the top CD layer can act not only as a blue luminescent emitter but also as a UV absorber along with a non-luminescent quencher, 2-(4-benzoyl-3-hydroxyphenoxy)ethyl acrylate (BHEA), for lanthanides. The thickness of the top layer, upon mechanical stretching, would decrease by the Poisson effect, resulting in enhanced transmittance of light to the bottom layer where the luminescence of the lanthanide was turned ON. Such mechanochromism can be tuned simply by changing the concentrations of CD or BHEA in the top-layer. These mechanochromic polymers have been demonstrated to be useful in pressure and contact force sensing as well as material-based encryption devices.

Other than lanthanides, hybridization of other transition metals in polymers possibly endows interesting stimuli-responsive luminescent properties. Such responsiveness is twofold. On one hand, upon the coordination of metals, fluorophores show fluorescence quenching or enhancement.[90–92] This mechanism has been often used in molecular systems for metal cation detection where fluorescent molecules alter their emission with metal coordination. An obvious case is charge or electron transfer from fluorophores to paramagnetic metal cations, like Cu^{2+} and Hg^{+}, leading to fluorescence quenching.[93,94] When incorporating those fluorophores in polymers, signal amplification through large conjugation systems could improve the sensitivity of those sensors.[95] On the other hand, adding metals can populate triplet states. Triplet emitters are known to efficiently enhance the light-emitting quantum yield,[96,97] for example in electroluminescence theoretically up to 100% efficiency. Although the details of the mechanism of metal–ligand charge transfer (MLCT) will not be discussed here, the add-in polymer can endow interesting responsiveness to those luminescent hybrids. In particular, the triplet state of those metal-containing polymers shows responsive phosphorescence.[98,99]

Other metal cations like Pt^{2+}, Ir^{2+} and Au^{+} can also show MLCT and enable phosphorescence[97,100] in metal–polymer hybrids. For instance, when simply coordinating with poly(4-vinylpyridine) (P4VP), $Au(C_6F_5)^{+}$ presents strong green emission, while both P4VP and $Au(C_6F_5)^{+}$ are non-emissive.[100] Although soft Au^{+} and hard N ligands are not incompatible, P4VP could enhance the formation of aurophilic interactions in the form of Au(I)···Au(I), both intra- and interchain. The hybrids have a photoluminescence quantum yield of 63%. In the solid state, those metal–polymer hybrids showed reversible mechanochromic luminescence between green and yellow-green emission.[101]

3. Self-healable metal/polymer hybrids

Self-healable or self-repairable materials can repair themselves upon mechanical damage. The most obvious example is the skin, which undergoes self-healing upon minor cuts. For synthetic materials, similar healing properties would improve the lifetime of materials, which is of particular importance for cross-linked polymers, like rubbers. Self-healable polymers are usually built with dynamic bonds that can be broken and reformed reversibly.[102–105] Those dynamic bonds can be either covalent, like dynamic covalent bonds,[106,107] or non-covalent, like hydrogen bonding,[108,109] p–p stacking,[110] hydrophobic interactions,[111–113] and coordination.[114–117] Most of those dynamic bonds rely on the design of well-defined molecular structures and their interactions are not changeable once the synthesis of polymers is fixed. In other words, to vary the strength of those covalent or non-covalent interactions, new synthesis is usually needed. As a comparison, coordination is among the most feasible to vary interactions used in self-healable polymers. The choice of different metals can lead to possible changes in the on-demand M–L coordination strength in a broad range.

Coordination is one of the most promising non-covalent interactions for the design of self-healable polymers.[118–121] First of all, metal–ligand coordination is highly tunable in terms of the binding strength as mentioned. The common binding motifs, such as N and O, vary their coordination affinity or K_b.[122] For example, pyridine- or phenol-containing ligands show tunable binding affinity to metals in response to pH. The deprotonated forms of pyridines and phenolates are usually strong ligands to transition metals, while their protonated forms are fairly weak. The change in binding affinity plays a determining role in the polymer chain dynamics, which controls the chain diffusion and eventually the self-healing efficiency. Second, metal–ligand coordination is strong to prepare mechanically stiff polymers. In the example of ferric–catechol complexes, K_b is in the range of 10^{10} to 10^{40} L mol^{-1} depending on the pH.[123] Large K_b results in the formation of strong binding close to covalent bonds. Some metal ions also have large coordination numbers[23] or form nanoclusters[124] to create high cross-linking density. Lastly, the metal endows new functionalities not existing in organic polymers, like luminescence and redox properties.[125] Taking Fe^{3+}/Fe^{2+} as an example, citrate can reduce Fe^{3+} to Fe^{2+} in the presence of UV light.[126] In the presence of hydrophilic ionic polymers like poly(acrylic acid) (PAA), Fe^{3+} can bind three carboxylates while Fe^{2+} only binds to two carboxylates. When reducing Fe^{3+} to Fe^{2+}, the lowered cross-linking density would induce a clear gel–sol transition of PAA solution. It is also possible to design photolabile coordination, which endows light responsiveness to metal/polymer hybrids.[127–129]

3.1 Bio-related self-healing (Fe^{3+} and Ca^{2+})

In bio-related self-healing applications, the mostly commonly used metal cations are Fe^{3+} and Ca^{2+}.[26,118,130–137] Fe^{3+}–catechol coordination has been identified from the byssal threads of mussels.[133,134,138–140] The byssus contains a protein family rich in tyrosinases which can be converted to catechols through hydroxylation. Abundant catechols can bind a variety of metal ions in minerals. K_b is as large as 10^{40} L mol^{-1}.[27,123] The tris- and bis-catochol–Fe^{3+} complexes are fairly stable. The single molecule tensile test shows that the rupture force to break catochol–Fe^{3+} binding is 0.8 nN (Fig. 5a), comparable to that of a covalent bond, ~2.0 nN.[118] More importantly, the metal–catechol complexes can reform upon breakage and such a dynamic property enables the self-healing of mussel byssal threads.[131,141,142] There has been a large volume of studies on bioinspired coordination Fe^{3+}–catechol to design hybrids with excellent mechanical strength and self-healing capability.

The binding strength and coordination number of Fe^{3+}–catechol complexes increase with pH,[135,143,144] although it is possible to form hydroxides under strong alkaline conditions. Waite's group has designed dynamic materials in the forms of hydrogels and elastic films using catochol–Fe^{3+} coordination. Using 4-arm PEG terminated with a catechol at each arm, they demonstrated self-healing polymer hydrogels with pH-controlled Fe^{3+}–catechol binding strength.[27] The binding stoichiometry of Fe^{3+}–catechol was adjusted by the pH through the de-protonation

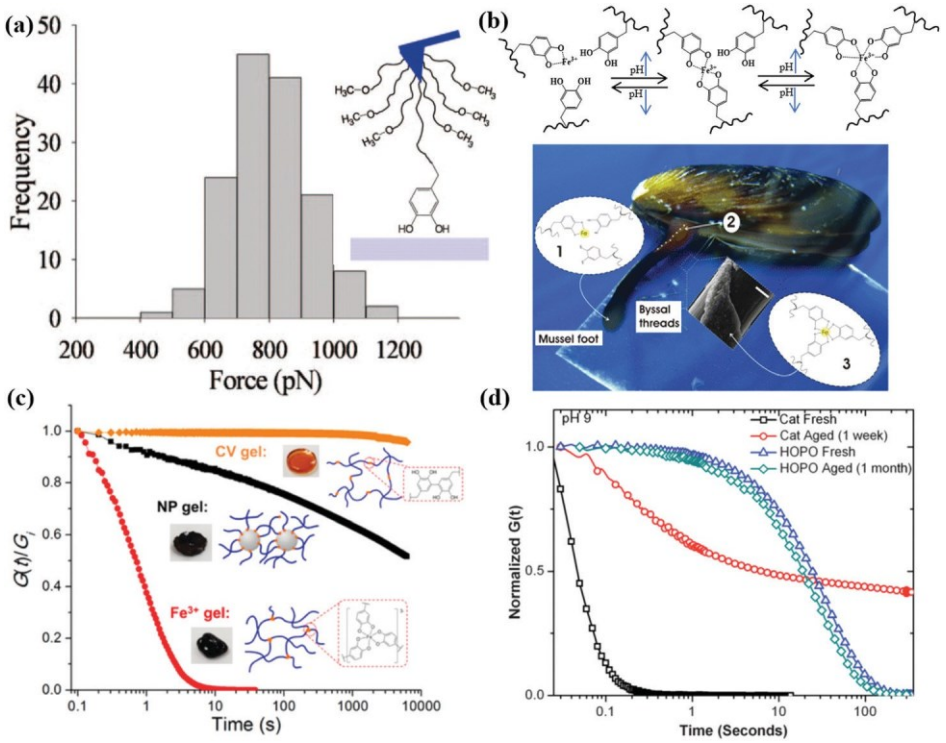

Fig. 5 (a) The plot of frequency versus pull out force for the dopa to metal surface. (b) The cross-linking mussel inspired Fe^{3+}–catechol containing polymers and their pH responsive Fe^{3+}–catechol coordination. (c) Step strain relaxation time of the intercatchol covalent crosslinking (CV) gel, Fe_3O_4 nanoparticle gel and Fe^{3+}–catechol crosslinked gel. (d) Relaxation time test to characterize the stability of the catechol and HOPO hydrogels. Figure (a) reproduced from ref. 118, copyright (2006) National Academy of Sciences, USA;[118] figure (b) reproduced from ref. 27;[27] figure (c) reproduced from ref. 119, copyright 2016 American Chemical Society;[119] figure (d) reproduced from ref. 120, copyright 2013 The Royal Society of Chemistry.[120]

of catechols (Fig. 5b). At pH ⌜ 5, the mono-catechol–Fe^{3+} complex was dominant and it did not cause the cross-linking of the polymer. A green/blue fluid was observed. When raising the pH to B8 at which the bis- or tris-catechol–Fe^{3+} complexes formed, a sticky purple gel was obtained. At pH B 12, tri-catechol–Fe^{3+} was favorable to result in the formation of a red elastic gel. The cross-linked Fe^{3+}–catechol hydrogels were self-healable, while the covalently cross-linked hydrogels by $NaIO_4$-induced oxidation of catechol were not healable.

When using polymeric ligands to bind Fe^{3+} ions, fast gelation usually results in heterogeneous polymeric networks and defective coordination. This often results in mechanically weak hydrogels. One possible solution is to pre-form the coordination complexes prior to polymerization. For example, polymerizable ligands, like dopamine methacrylamide, were chelated with Fe^{3+} ions first.[145] Further polymerization could lead to the formation of dense networks with high mechanic strength without decreasing the self-healing efficiency. Dopamine with a simiar catachol group could bind with $FeCl_3$ at pH from 8–10. The formed bis- or tris-catechol–Fe^{3+} complexes had distinct absorption features. The bis-catechol–Fe^{3+} complexes formed at pH 8 had a maximum absorption peak at 535 nm, while that of the tris-catechol–Fe^{3+} complexes formed at pH 10 was at 467 nm. At both pHs, it allowed a maximum use of coordination between catechol and Fe^{3+} to decrease the coordination defects. After photopolymerization, highly elastic hydrogels could be yielded. With the tris-catechol–Fe^{3+} complexes, the hydrogels had a strain of 1000% at break in a tensile test, and that of the hydrogels with the bis-catechol–Fe^{3+} complexes was 800%. Both hydrogels were self-healable within 20 min. After healing a maximun strain of 800% was achieved before rupture for the hydrogels with the tri-catechol–Fe^{3+} complexes.

There are a number of studies on balancing the self-healing efficiency and the mechanical strength of hydrogels formed by catechol–Fe^{3+} complexation. For example, instead of Fe^{3+} ions, Fe_3O_4 nanoparticles can bind with catechol as well, while the network formed by catechol–Fe_3O_4 complexation shows completely different relaxation mechanics.[119] With nanoparticles as cross-linkers, the stress relaxation was much slower where there were orders of magnitude more chains involved (Fig. 5c). In addition, Fe^{3+} is a strong oxidant and it can oxidize catechol in air and thus chemically cross-link hydrogels. Through modifying catechol with strong electron-withdrawing groups on the aromatic ring, the oxidation of catechol can be significantly slowed down. For example, Waite's group designed catechol derivatives, e.g., 4-nitrocatechol and 3-hydroxy-4-pyridinonone (HOPO), to bind Fe^{3+} ions.[120] The hydrogels made from HOPO–Fe^{3+} complexes showed long-term stability for months without changing their rheological and dynamic characters (Fig. 5d).

Another example of bio-related metal ions for self-healing applications is Ca^{2+}. Ca^{2+} as an essential metal in biology is multi-functional, such as in signal transduction, enzymes and

biomineralization.[146] Early studies in alginate gels suggested that divalent Ca^{2+} ions interacted electrostatically with carboxylates of alginate to form hydrogels.[147–149] Those biocompatible hydrogels are not toxic for proteins and cells and they have been used for immobilization of enzymes and cells. Bisphosphate shows high binding affinity to Ca^{2+} ions or other Ca^{2+}-containing nanoparticles as inspired by hydroxyapatite in living bones.[150–152] Using polysaccharide hyaluronic acid (HA), bisphosphate ligands can be introduced through EDC [1-ethyl-3-(3-dimethylaminopropyl)carbodiimide] coupling. Ca^{2+} ions can cross-link through binding with bisphosphate to form self-healable hydrogels. Nevertheless, the binding or the electrostatic interaction of alkaline metals with ligands is fairly weak. The mechanical strength of those hybrid gels is often weak.

3.2 Other metals in self-healing

In terms of the network strength, lanthanides are among the best choice of metals given their large radius and coordination number. They are able to bind 9–12 ligands per metal ion, possibly improving the mechanical strength of hybrids. Bao and co-workers designed Eu^{3+}-containing polyurethane elastomers with b-diketone binding motifs (Fig. 6a).[53] Using naturally produced curcumin, copolymerization with isophorone diisocyanate, poly(tetramethylene ether glycol) and 1,4-butanediol yielded polyurethane with diketone on the backbone. The addition of Eu^{3+} could improve the moduli close to two orders of magnitude at low frequency. When the molar ratio of b-diketone to Eu^{3+} reached 3 : 1 (mol), the tensile strength of the hybrid elastomer reached 1.8 MPa with 900% strain at break. In the meanwhile, there was no obvious increase in tensile strength with other metals, like Cu^{2+}.[53] Eu^{3+}-Containing polyurethane elastomers showed spontaneous self-healing at room temperature. The healing efficiency estimated from the restoration of the tensile strength reached 98% after 48 h.

The choice of the counterions seems to play an important role in the self-healing efficiency as well. Using bipyridine-containing polydimethylsiloxane (PDMS, Fig. 6b), Bao's group showed the importance of counterions to the self-healing

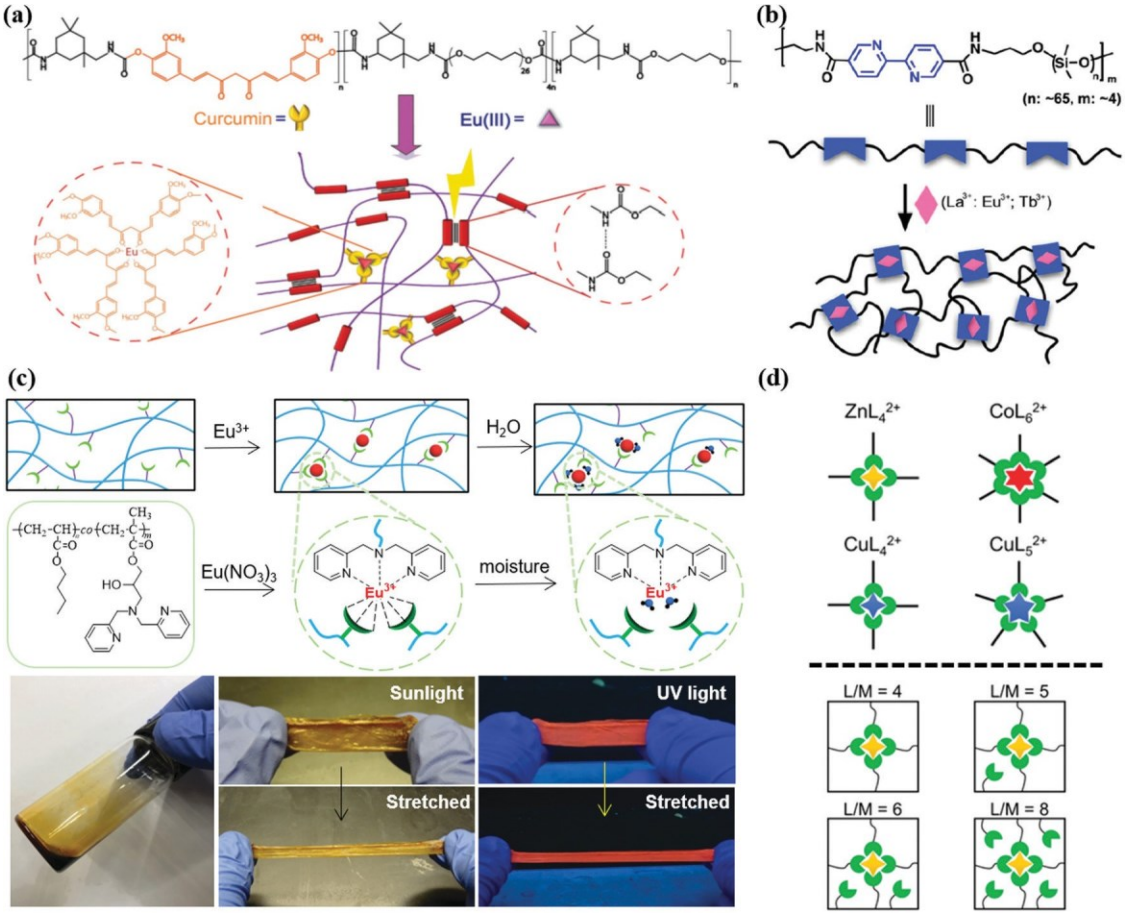

Fig. 6 (a) Scheme showing the structure of Eu^{3+}-containing polyurethane elastomers with b-diketone binding motifs. (b) The synthesis process to prepare bipyridine containing polymers and preparation of metal containing elastomers; the bottom scheme illustrates the proposed ligand and counter ion effects. (c) The mechanism of using moisture to control Eu–DPA coordination in P(nBA-co-GMADPA). Pictures showing the pristine state of P(nBA-co-GMADPA) and the self-standing film under sunlight or under UV light. (d) The imidazole containing polymer coordinated with different transition metals and the topology effects on the mechanical properties. Figure (a) reproduced from ref. 153, copyright 2019 Wiley VCH;[153] figure (b) reproduced from ref. 154, copyright 2017 Wiley VCH;[154] figure (c) reproduced from ref. 45, copyright 2020 The Royal Society of Chemistry;[45] figure (d) reproduced from ref. 155, copyright 2016 American Chemical Society.[155]

ability of hybrid films.[154] Different counterions like trifluoromethanesulfonate (OTf^-) and nitrate (NO_3^-) for Eu^{3+}/Tb^{3+} were compared in parallel in terms of the chain mobility and self-healing behavior at room temperature. Triflate lanthanide salts were found to be stronger cross-linkers and to improve the toughness and elasticity. The PDMS film crosslinked by Eu^{3+}/Tb^{3+} with OTf^- showed healing efficiency >90% while the $Eu(NO)_3$ and $Tb(NO)_3$ containing films showed <20%. Small angle X-ray scattering (SAXS) suggested that the film with lanthanide triflate increased the domain size compared to that of the elastomer having lanthanide nitrate. This enhanced the chain mobility and resulted in the improvement of the healing efficiency.

Although a high cross-linking density improves the mechanical strength of hybrid films, this shows a great impact on the chain dynamics. There is a trade-off between the chain dynamics and the mechanical strength of hybrid films. With lanthanides, one possible solution is to use competitive molecular ligands, such as water, to trigger fast self-healing, and then the competitive ligands can be removed to restore the mechanical properties. Our group recently designed an Eu^{3+}-containing elastomer consisting of poly(n-butyl acrylate) (PnBA) incorporated with 2-hydroxy-3-dipicolylamino methacrylate (GMADPA) (Fig. 6c).[45] With 15 mol% of GMADPA, the copolymer with a low Eu-to-DPA ratio of 1 : 7 formed elastic and self-standing films. The film was stretchable and red-emissive. GMADPA has dipicolyamine moieties as a tridentate ligand with three N atoms to bind Eu^{3+} ions. However, water as a preferred ligand for Eu^{3+} can compete with dipicolyamine. In the presence of trace amounts of water, the disruption of Eu^{3+}–DPA complexes was seen, leading to (i) significant luminescence quenching of Eu^{3+} ions and (ii) lowering of the moduli of the hybrid film. The self-healing efficiency of the hybrid film was improved by roughly 100 times in the presence of moisture, while the mechanical robustness could be recovered after removal of water.

The M–L coordination dynamics can also be varied by other stimuli, e.g., light. For Ru complexes, ligand substitution and exchange can be triggered by the change in the ligand field in photoexcited states.[156] For example, in $[Ru(terpy)(phen)(L)]^{2+}$ (terpy: 2,2′;6′,2″-terpyridine; phen: 1,10-phenanthroline; and L is a thioether or other weak ligands), the weak L ligand can be photocleaved and replaced by water upon excitation with light,[157] while the unstable Ru–H_2O can return to the thermodynamic stable Ru–thioether form in the dark. Wu and coworkers demonstrated the use of photocleavable Ru–thioether binding in light-triggered fast self-healing gels.[158] Using polymerizable pentacoordinated Ru complexes with (2-(2-(2-(methylthio)ethoxy)-ethoxy)ethyl acrylate) and N-hydroxyethyl acrylamide, organohydrogels could be prepared in H_2O/glycerol mixtures with a concentration of Ru complexes of ~1 mol% relative to N-hydroxyethyl acrylamide. Such organohydrogels showed interesting light-triggered sol–gel transitions. Upon exposure to green light (530 nm, 10 mW cm^{-2}), the organohydrogels became fluidic after 5 min irradiation as a result of the cleavage of Ru–thioether cross-linkers. The gel state could be recovered when storing the liquid in the dark after 25 min. The organohydrogels allowed the reversible sol–gel transition to occur even at −20 1C. Those organohydrogels were healable on a similar timespan as triggered by light irradiation. Light as a trigger provides spatial control of the healing region where the gel-to-sol transition could be induced locally for rapid recovery.

Other than the coordination strength, the coordination geometry of transition metals also plays a role in the self-healing behaviors of hybrid films.[159–170] The coordination geometry of metals determines the number of ligands and further the chain dynamics, which are tunable by the chemical nature of the ligands.[28,165,169,171,172] The mechanical properties and self-healing behaviors of hybrid films were influenced by the choice of metals as demonstrated by Guan's group.[155] Using imidazole-containing brush polymers of PnBA and polystyrene (PS), three different metals, i.e., Co^{2+}, Zn^{2+} and Cu^{2+}, with a similar ionic radius and electrostatic charge, were incorporated to investigate their impact on the solution and bulk film properties (Fig. 6d). Zn^{2+} and Cu^{2+} ions showed more dynamic behavior where the brush polymers had no changes in viscosity and elasticity with low metal loading (metal-to-ligand ratio <1 : 4), but there was a sharp transition with a further increase in metal loading. For Co^{2+}, there was a proportional increase in the viscosity of the polymer solutions and melts. The tetrahedral complexes, such as Cu^{2+} and Zn^{2+} with imidazole, were thought to have fast ligand exchange compared to that of octahedral Co^{2+}, where the ligand exchange rate was independent of the concentration of free imidazole. The large difference in coordination geometry and dynamics had a similar impact on the self-healing efficiency. The Zn^{2+}-containing brush polymers showed 90% healing after 3 h,[173] while it was less than 30% for the Co^{2+}-containing polymers. The ligand exchange dynamics therefore determines the diffusion rate of polymer chains, which dominates the self-healing efficiency.[155] Similarly, in bipyridine-containing PDMS, Zn^{2+} showed fast self-healing compared to Fe^{2+}.[116]

M–L coordination alone as physical cross-linking in polymers usually is still too weak to yield self-healing materials with high mechanical strength. Another possible solution is to combine M–L coordination with other non-covalent interactions like hydrogen bonding and hydrophobic interactions. The formation of two networks can significantly improve the mechanical strength of polymers (see Section 4). Since both networks are formed by non-covalent interactions, those hybrid polymers are self-healable. For example, bi-functional acrylate, 2-(3-(3-imidazolylpropyl)ureido)ethyl acrylate (IUA), is polymerizable. It provides hydrogen bonds through ureido and M–L coordination through imidazole. Using random copolymers with PnBA, Zn^{2+}–imidazole complexation could improve the tensile strength by ~40 times.[28] The film was healable upon heating up to 88% after 48 h. Yamaguchi and coworkers prepared copolymers of poly(d-valerolactone)–poly(lactic acid) (PVL–PLA) containing ligands of 2,2-bipyridine and hydrogen bond sites of 2-ureido-4-pyrimidinone.[174] Three metal ions of Zn^{2+}, Co^{2+} and Fe^{2+} could be incorporated into the polymeric networks. The films with double networks had a high toughness, e.g., ~85 MJ m^{-3} of the Fe^{2+}-containing films, 3.5-fold higher

than that of the metal-free films. The hybrid films also showed a reasonable healing efficiency up to 77% after annealing at 50 1C for 30 min.

4. Tough elastic metal/polymer hybrids

The toughness, defined as the amount of energy dissipation before a material is broken, is an important measurement of the fracture-resistance of a material. Previous studies on elastic polymers including hydrogels and elastomers suggest that, when building two interpenetrated, covalently cross-linked networks in elastic polymers, the toughness of the elastic polymer can be improved significantly.[175–181] In these interpenetrated or double-network polymers, the two different networks are very different from each other in terms of the strength.[176,178] One network is usually weaker (low fracture stress, dense network) and more brittle (low extensibility) than the other network. Upon stretching, the weaker network ruptures first, while the second stretchable network retains the integrity of the elastic polymers. The rupture of the weaker network dissipates a large amount of energy (i.e., the work done by stretching) to avoid any damage of the second network. This endows interpenetrated or double-network polymers with high toughness. An alternative design to toughen those elastic materials is to build weak networks with non-covalent interactions.[24,182–189] As such, the stronger network, e.g., made from covalent cross-linking, mainly contributes to the mechanical robustness (high modulus), while the other network, e.g., made from non-covalent cross-linking, dissipates energy through reversible dissociation upon deformation (high elasticity).[190] In the stress–strain curves, tough materials usually show a distant yield region where the weak network starts to break down and the loose but strong network retains the integrity of the polymers. When both networks are made with chemical cross-links, the loss of such toughness is permanent because the disrupted network is not recoverable. If the brittle network is built with non-covalent interactions, the toughness of those elastic polymers is recoverable upon the reformation of those non-covalent interactions.

Dynamic M–L coordination is among such non-covalent cross-links to build up tough elastic hybrids. The strength of coordination complexes as measured by $DG_{complex}$ varies from very weakly chelating systems to strongly chelating M–L (~100 kT) pairs like catechol–Fe^{3+}.[27] The dynamic cross-links make the brittle network reversible and add-in large energy dissipation. In typical preparation of tough elastic polymers, weak M–L complexation can be added before the formation of covalent cross-linking in the polymers. Suo and co-workers reported the preparation of tough and highly stretchable hydrogels using chemically cross-linked ionic polymers together with weak ionic interactions.[182] Alginate, as discussed in a previous section, binds with divalent cation Ca^{2+} through weak coordination/ionic interactions with carboxylate. In polyacrylamide hydrogels, the addition of alginate and calcium sulphate induced a weak physical cross-linking network together with the hydrogen bonds among alginate. After photopolymerization to chemically cross-link acrylamide with N,N-methylenebisacrylamide, highly stretchable and tough hydrogels could be obtained. Despite having 86 wt% water, the hydrogels could be stretched ~20 times their initial length with a fracture energy of 8700 J m^{-3}, while the parent hydrogels of alginates and polyacrylamide only show a fracture energy of 10–250 J m^{-3}. The hydrogels were also notch-insensitive and up to 1700% strain at break was seen for the films with notches. When stretching the hydrogels with two networks, the polyacrylamide network formed by chemical cross-links remained intact and the alginate network unzipped gradually. The breaking of non-covalent interactions of alginate–Ca^{2+} dissipated the energy and the hydrogels showed large hysteresis. The non-covalent binding of alginate–Ca^{2+} could restore and then heal the weak networks as well as the toughness of the polymer hydrogels. Such hybrid hydrogels are ideal as a model system to design tough elastic materials and explore mechanisms of deformation and energy dissipation.[53,185,187,188,191–197]

The toughness of elastic materials consisting of covalent and non-covalent networks is recoverable since the weak interactions and also the non-covalent network are reversible. However, such recovery of toughness is kinetically slow. In the first report from Suo's group, the recovery of toughness was around 74% after 24 h. The immediate cycle of loading/unloading would result in much weaker hydrogels. A possible solution is to use dynamic covalent bonds to build up the strong network. Dynamic covalent bonds are strong enough to retain the macroscopic shapes of the films/hydrogels under high strain, while they endow faster chain kinetics to rezip the non-covalent interactions and to restore the double networks. When combining dynamic covalent cross-links, the tough elastic materials are also self-healable. Ghanian et al. demonstrated tough hydrogels with fast recovery of toughness using double networks formed by a Diels–Alder reaction and alginate–Ca^{2+} binding. For alginate, partial substitution of the carboxyl groups with furan could couple with four-arm PEG-maleimide (4arm-PEG-Mal).[198] The Diels–Alder reaction of 4arm-PEG-Mal and alginate occurred under UV-vis irradiation and chemically cross-linked the hydrogels. The toughness of the hydrogels was tunable by controlling the substitution degree of furan on alginate. With a 20% furan substitution degree, the hydrogels had a toughness of 136.7 J m^{-3}. Such hydrogels had a set of interesting features such as fast self-recoverable toughness and self-healing upon rupture. Even after immediate reloading, the toughness of the hydrogels was fully recovered.

Changes in coordination strength possibly improve the mechanical properties of tough elastic hybrids. For example, when using lanthanides in the weak, non-covalent networks, the hydrogels are tough, photoluminescent and mechanically strong. Eu^{3+}–alginate and polyacrylamide hydrogels had a tensile strength of 1 MPa with an energy dissipation of ~9000 kJ m^{-3} at a maximum strain of 2000%.[186] In the hydrogels of Eu^{3+}–alginate and poly(vinyl alcohol) (PVA), the resultant hydrogels exhibited high mechanical strength as well, e.g., ~7 MPa in compressive strength and 900 kJ m^{-3} energy dissipation under 400% stretch. In addition, with lanthanide ions, those hydrogels were strongly photoluminescent

and showed antibacterial activity.[183] Hong et al. have compared the impact of metal cations on the mechanical strength of the polyurethane elastomer.[199] With Eu^{3+} ions, the elastomer had a tensile strength of 15.2 MPa at break of 1053% strain and a toughness of 59.1 MPa as the area under the stress–strain curve. With Zn^{2+}, the elastomer film had a tensile strength of 9.5 MPa at break of 1450% strain and a toughness of 50.5 MPa. The improvement in the tensile strength and toughness was a result of intermolecular cross-linking by metal cations with lager coordination numbers.

In the case of lanthanides, the toughness of hybrid films is stimuli-responsive as the coordination of lanthanide ions is responsive to water as discussed previously. When the weak network can be turned ON or OFF, the mechanical behavior is therefore shapeable. In the presence of M–L coordination, tough elastic mechanics is expected as the coordination dissipates the energy. When further weakening the coordination, the toughness can be removed to form ''soft'' elastic materials. Our group demonstrated this strategy using dynamic coordination of Eu^{3+}–IDA as a key component to build up the physical cross-linking network in the elastic films consisting of interpenetrated networks. We used chemically cross-linked poly(acrylic acid-co-n-butyl acrylate) by ethylene glycol dimethacrylate as the strong network and iminodiacetate-containing poly(di(ethylene glycol)-methyl ether methacrylate) ($PMEO_2MA$) to coordinate Eu^{3+} ions as the weak network (Fig. 7a).[24] After removal of the solvent, highly elastic films could be prepared. The reversible dissociation and reformation of the Eu^{3+}–IDA complexation could dissipate energy very efficiently. Even with a low content of Eu^{3+} ions (a mole ratio of IDA-to-Eu of 7/1), the modulus of the tough polymer film reached 24.3 MPa (Fig. 7b), one order of magnitude higher than that of the film without Eu^{3+} ions.[24] The energy dissipation of the first cycle reached ~1500 kJ m^{-3} at 200% strain (Fig. 7d). The coordination network underwent fast recovery where ~900 kJ m^{-3} energy dissipation was seen immediately after reloading. The toughness and photoluminescence were responsive to moisture. Under 80% relative humidity, the hybrid polymer film was ''soft'' elastic without any yielding point along with the significant weakening of its red emission (Fig. 7e and f). Both the mechanical states and photoluminescence were restored after removing the moisture from the film. The in situ dynamic mechanical test indicated that the storage modulus of the hybrid films decreased with purging moisture and the films showed a more significant viscous property. The storage modulus recovered after removing the moisture within 25 min where the elastic solid state could be restored as well.

The balance of material toughness and strength is somewhat similar to that in self-healing. Solely increasing the mechanical strength usually leads to the formation of more brittle and less elastic materials. Valentine and co-workers

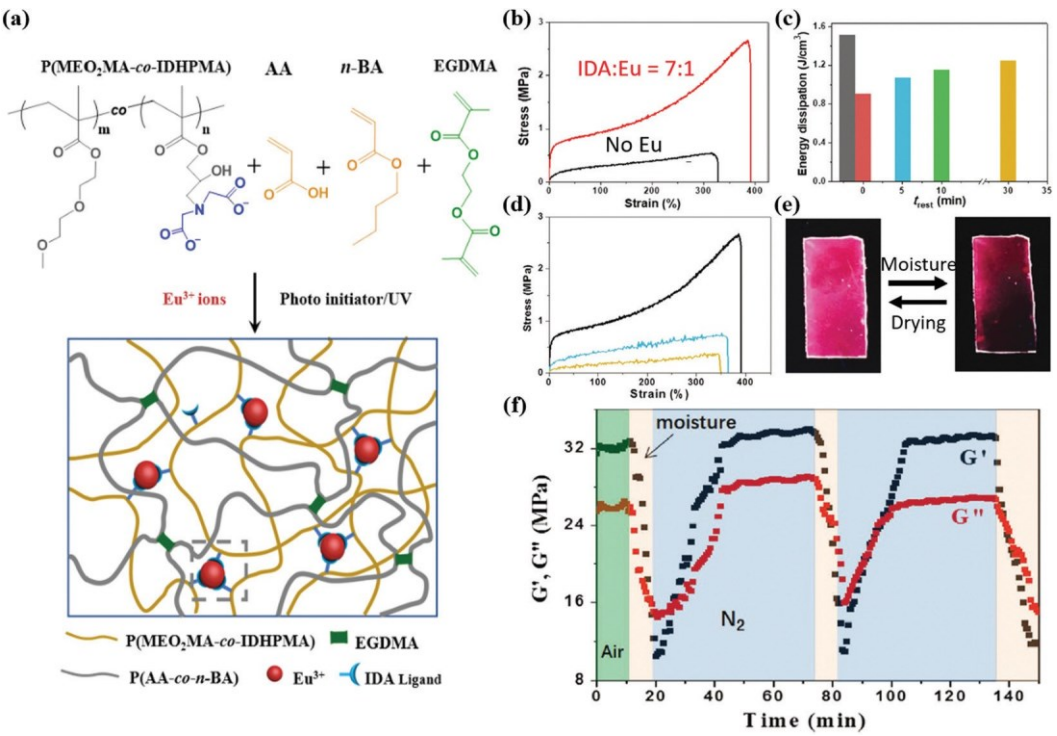

Fig. 7 (a) Illustration of the network structure of the IPN tough elastomer. (b) Tensile stress curves of the elastomer without Eu^{3+} ions (black) and the Eu^{3+}-containing elastomer (red). (c) Histogram of toughness calculated from cyclic loading with a maximum strain of 200%. From left to right denotes the first to fifth cycle. The second to fifth cycles have a rest time (t_{rest}) of 0, 5, 10, and 30 min, respectively. (d) Stress–strain curves of the Eu^{3+}-containing polymer films subject to 0 h (black), 1.5 h (blue) and 2.5 h (orange) of moisture at a relative humidity of 80%. (e) Images showing the reversible luminescence ON/OFF response of the elastomer film triggered by moisture at room temperature. (f) Moisture-driven switch between elastic solid and viscous fluid states of the elastomer by a dynamic mechanical measurement in a closed chamber alternatively purged with N_2/water-saturated air. Figures reproduced from ref. 24, copyright 2019 Wiley VCH.[24]

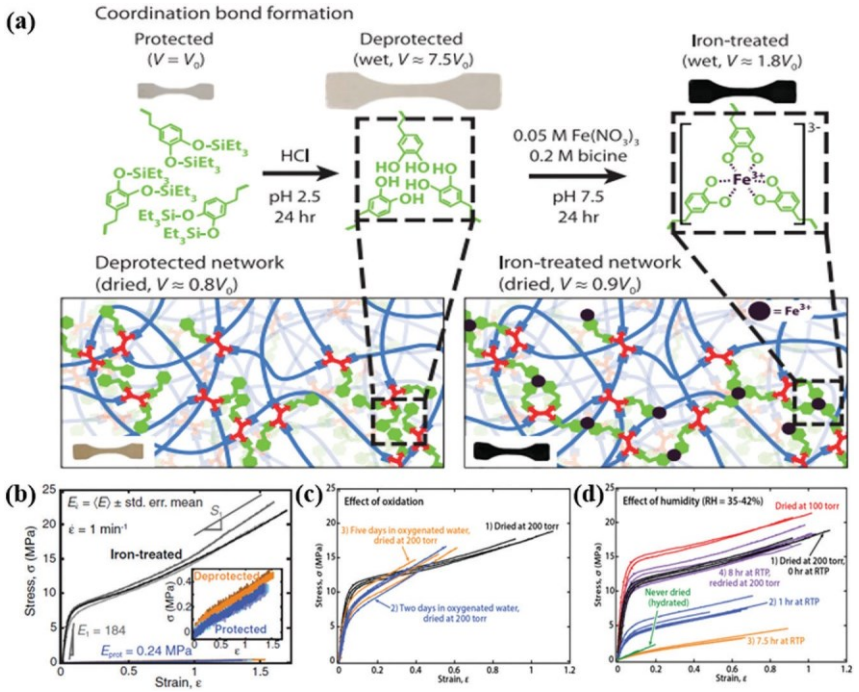

Fig. 8 (a) Image showing the protected and deprotected network, the cross-linking network prepared with Fe^{3+}–catechol and the illustration of the swelling test specimen during the process. (b) Stress–strain curves of protected (blue), deprotected (orange), and iron-treated samples (grey) with a strain rate of 1 min^{-1}. (c) The effect of oxidation on the mechanical property of the sample. (d) The influence of humidity on the stress–strain relationship of the sample. Figures reproduced from ref. 136, copyright 2017, Science.[136]

demonstrated that the use of catecholate–Fe^{3+} coordination could possibly offer a solution to balance the strength and toughness (Fig. 8a).[136] In the amorphous epoxy with loosened chemical cross-links, triscatecholate–Fe^{3+} complexation was designed through mild deprotection under low pH to avoid catechol–catechol oxidative coupling. Triscatecholate–Fe^{3+} formed a stable but dynamic network. With this strategy, the dry elastomer had a Young's modulus of 184 MPa while retaining good stretchability with a maximum strain of ~150% (Fig. 8b). The polymers with a triscatecholate–Fe^{3+} coordination network showed a 58-fold higher tensile strength than the pure polymer and the elastic modulus increased by 770-fold after introducing Fe^{3+} ions. As a comparison, the stiffness and extensibility of the tough elastomers were weakened under oxidative conditions and high humidity, which swells the Fe^{3+}-rich domains (Fig. 8c and d).

There has been a large volume of work on metal-toughened natural and synthetic rubbers.[200–203] Most of those rubbers are chemically cross-linked by sulfur or chemicals. Adding in M–L coordination as a sacrificial network could possibly toughen those materials. Guo and co-workers demonstrated that incorporating M–L coordination into rubber enhances the mechanical stiffness as well as the toughness of rubber materials. For example, for styrene–butadiene rubber containing vinylpyridine, a small amount of Zn^{2+} ions could lead to the improvement of the tensile strength and toughness without a significant change in elasticity.[202] Sacrificial M–L coordination dissipates a large amount of energy, which enhances the toughness of the rubber materials.

5. Catalysis using metal/polymer hybrids

While most synthetic polymers are not catalytically active by themselves except in acid–base hydrolysis, catalytically active metals can be supported on synthetic polymers. Loading expensive metal catalysts on insoluble polymer beads or films offers a valuable way to recycle and recover those catalysts. The rationale for using those polymer-supported metal catalysts is to reduce the cost of expensive catalysts and increase their lifetime. There are quite a few excellent reviews with a focus on polymer-supported metal catalysts.[8,204–206] The question of this section we would like to address and summarize is whether synthetic polymers contribute to the catalysis of metals, like the catalytic efficiency and selectivity.[207] The ideal role of polymers in catalysis is twofold. First of all, synthetic polymers work as the second coordination sphere of metals to control the access of substrates. The early studies on core-functionalized dendrimers suggest that the branched chains of dendrimers can tune the accessibility of metals confined in the core of dendrimers.[208–210] Later examples on stimuli-responsive polymers show that the reversible change in the coil-globular confirmation can turn ON/OFF the catalytic activity of metal ions/nanoparticles.[211–214] Second, polymers provide an "ensemble" environment to metals that varies the local pH, the concentration of protons, the hydrophobicity and the number of metal sites. The impact of the polymer could be different from reaction to reaction, but it is highly engineerable on demand for any given specific reaction.[215–217] For example, polymers with multiple binding motifs can bring a number of metal sites in one

polymer chain with identical coordination chemistry.[218,219] Those metal/polymer hybrids show better activity for reactions catalyzed by multiple metals cooperatively, as compared to monomeric coordination metal complexes. In addition, synthetic polymers as a support offer better stability to metal ions/nanoparticles during reactions, largely increasing the lifetime of hybrid catalysis.[220,221]

5.1 Polymer-promoted catalysis

Dendrimers and other branched polymers have historically received broad interest. Dendrimers with well-defined branched structures offer precise control over the location and number of active sites. Metal-containing dendrimers usually with multiple active sites on nanosized molecules are considered to bridge the study of homogeneous and heterogeneous catalysis. Depending on the location of metals, there are two different metal-containing dendritic catalysts, including periphery- and core-functionalized dendrimers where the metal sites are present on the surface and the core of the dendrimers, respectively.[222] Periphery-functionalized dendrimers support multiple metal sites, possibly promoting their catalytic activity, while core-functionalized dendrimers with usually one or two metal sites per molecule offer better spatial control of the metal sites.

Using low-generation dendrimers, periphery-functionalized dendrimers can separate multiple metal sites on the surface of the dendrimers, which nearly retains the activity of each metal site. Knapen et al. prepared silane dendrimers (G0 and G1) with homogeneous Ni^{2+} sites to catalyze Kharash addition of C–C bonds.[223] The turnovers per Ni^{2+} site were ca. 80% and 70% for G0 (four Ni^{2+} sites) and G1 (twelve Ni^{2+} sites), respectively, compared to that of mononuclear Ni^{2+} complexes (Fig. 9a and b). The dendritic effect on the catalytic efficiency usually varies in different reactions. In periphery-functionalized dendrimers, a positive dendritic effect is expected when there is cooperativity between terminal groups. For example, Ouali et al. studied the use of Cu-containing dendrimers to catalyze O- and N-arylation.[224] For the coupling of iodobenzene and 3,5-dimethylphenol, there was a weak dendritic effect for Cu-containing G1 and G2 catalysts where the yield of diarylether was comparable with the monomer Cu catalyst bound with bidentate N-[(1E)-pyridin-2-ylmethylene]-aniline. On the contrary, for the arylation of pyrazole with aryl halides (iodobenzne and bromobezene), the Cu-containing G1 and G2 catalysts had a significant dendritic effect. There was a ~20-fold higher yield for the dendritic Cu catalysts compared to that of the monomeric Cu catalyst. The higher generation dendrimers for both arylations were much more active than the monomer Cu catalyst. The dendritic catalysts also show unique kinetic enhancement of 2–3 orders of magnitude together with polyvalent substrates as demonstrated by Finn and coworkers.[225] Enhanced binding and rolling in polyvalent catalysts and substrates show very interesting dendritic effects on catalysis.

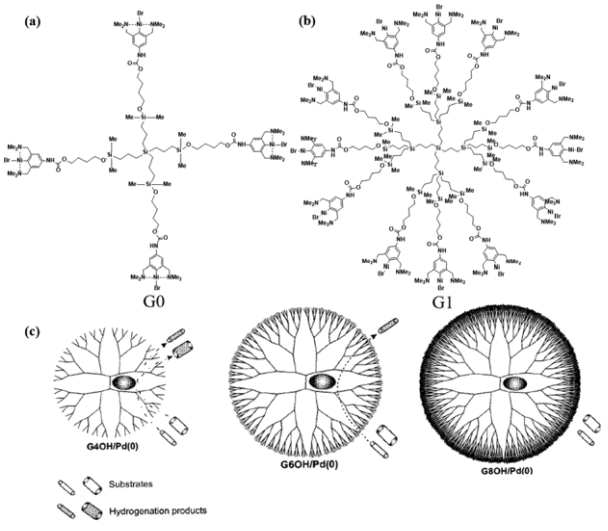

Fig. 9 Structure of Ni^{2+}-containing dendrimers, (a) G0 (four Ni^{2+} sites) and (b) G1 (twelve Ni^{2+} sites). (c) Scheme illustrating how the surface crowdedness of dendrimers limits the accessibility of Pd(0) and the catalyst. Figures (a and b) redrawn from ref. 223;[223] figure (c) reproduced from ref. 30, copyright 2001 American Chemical Society.[30]

In core-functionalized dendrimers, metal sites are confined by branched molecules that possibly control the accessibility of metal ions.[30,208–210] For example, steric crowding imposed by the dendrimer periphery controls the diffusion rate of substrates through the dendrimers, thus resulting in different reactivity on metals. Crooks and coworkers demonstrated that Pd nanoclusters (~1.7 nm) encapsulated in poly(amidoamine) (PAMAM) dendrimers showed size-selective hydrogenation of olefins.[30] Those tiny nanoclusters were synthesized with hydroxyl-terminated PAMAM dendrimers with different generations, G4, G6 and G8. By varying the generations of PAMAM dendrimers, the average distance between terminal hydroxyl groups was tunable, e.g., 8.2 Å for G4, 5.4 Å for G6 and 3.2 Å for G8. When increasing the size of the substrates, i.e., allyl alcohols, the accessibility became limited as a result of the bulkiness of the dendrimer periphery. There was a clear trend of the Pd catalytic activity correlated to the size of the substrates and the generation of the dendrimers. The maximum turnover frequency of Pd nanoclusters reached 480 mol H_2 h^{-1} per mol Pd for the simplest allyl alcohol using Pd in G4. For the same substrate, the turnover frequency of Pd dropped to 120 mol H_2 h^{-1} per mol Pd using G8. With Pd in G4, the turnover frequency for 3-methyl-1-penten-3-ol also dropped to 100 mol H_2 h^{-1} per mol Pd. The surface crowdedness therefore limited the interaction between the metal site and the substrate (Fig. 9c).

Once bound with polymers, the availability of metal catalysts is variable by changing the physiochemical properties of the polymers. Using synthetic polymers as ligands also endows unique responsiveness to the metal catalysts that does not exist in molecular complexes. For example, thermoresponsive polymers can shift their solubility and known critical solution temperature.[206] When bound with metals, those responsive polymers can inverse their solubility to control the metal–substrate binding. Bergbreiter and coworkers showed that thermoresponsive Pluronic block copolymers of poly(ethylene oxide)-b-poly(propylene oxide)-b-poly(ethylene oxide) (PEO–PPO–PEO) bound with Rh^{+} had anti-Arrhenius reactivity.[214] Modified by alkyldiphenylphosphine at two ends, PEO–PPO–PEO had a lower critical solution

temperature (LCST) around 25 1C. Rh^{+} bound with PEO–PPO–PEO was active when the polymer ligands were water-soluble. At 0 1C, a turnover frequency of 13 mole H_2 h^{-1} per mole Rh^{+} was received, while the catalyst was inactive above 25 1C where simply the polymer catalysts became insoluble. Similar, the change in polymer chain conformation varies the enantioselectivity of bound metals.[226] Single-handed helical poly(quinoxaline-2,3-diyl) showed solvent-dependent helix inversion. When bound with Pd^{2+}, hydrosilylation of styrene showed excellent enantioselectivity along with the change in the helicity of poly-(quinoxaline-2,3-diyl).

Unlike dendrimers, linear polymers do not have precise structures, e.g., chain length and chemical homogeneities; therefore, they do not provide exactly defined coordination environments to metals. As a result, there are profound heterogeneities when adding metals to linear copolymers due to the polydispersity of synthetic polymers. Recent studies showed that linear polymers can provide coordination environments to enhance the catalysis of metal sites, despite those heterogeneities. There are two reported mechanisms so far. The first one is the ''colligative'' effect, termed for the improvement of the catalytic properties of metal ions when incorporating them into polymers with multimetal sites in proximity. There are many reactions catalyzed by two or more metals cooperatively.[227] For example, multicopper oxidases, e.g., tyrosinases and ascorbate oxidases, have two or more Cu sites to activate oxygen cooperatively. Incorporating multicopper sites in polymers, as compared to monocopper complexes, confines the diffusion of catalytic sites and provides proximity to adjacent catalytic sites to improve such cooperativity. Our group has examined the ''colligative'' effect of polymeric type-3 Cu sites in oxygen activation (Fig. 10a).[218] Using a water-soluble linear copolymer of poly(N,N′-dimethylacrylamide-co-2-hydroxy-3-(dipicolyamino)-propyl methacrylate) (P(DMA-co-GMADPA)), Cu^{2+} could bind with the copolymers. Simply varying the monomer ratio of DMA and GMADPA, the concentration of Cu^{2+} ions per polymer chain was variable. Although Cu^{2+} ions showed identical coordination geometries with monomeric GMADPA and polymeric P(DMA-co-GMADPA), the reactivities were profoundly different. For the oxidation of two different substrates, e.g. 3,5-ditertbutycatchol and L-ascorbic acid, the polymeric Cu catalyst had a 6–8 fold reactivity enhancement in comparison with Cu–GMADPA. Using the Michaelis–Menten kinetic model, the Michaelis constant (K_M) was found to increase with the Cu concentration per chain. Despite the imposed thermodynamic barrier, the intramolecular cooperativity of polymeric Cu catalysts was found to enhance the activity of Cu sites.

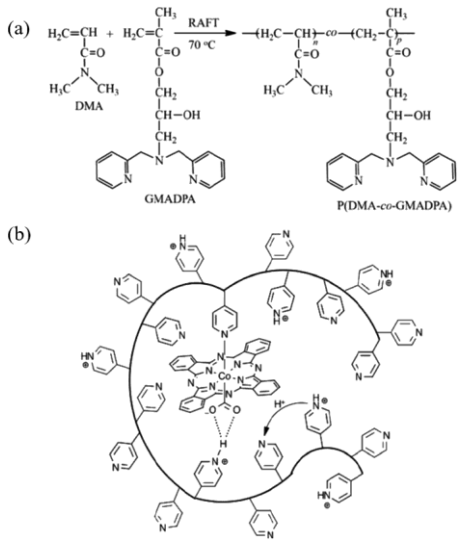

Fig. 10 (a) Chemical structure of P(DMA-co-GMADPA). (b) Scheme illustrating the outer coordination effects of P4VP on CoPC for CO_2 reduction. Figure (a) reproduced from ref. 218, copyright 2019 American Chemical Society;[218] figure (b) reproduced from ref. 215, copyright 2016 The Royal Society of Chemistry (open access).[215]

The second mechanism is the outer coordination sphere effect. The outer coordination sphere effect is well-known in molecular metal catalysts where adding functional groups with no direct binding with metal sites varies the activity of metals. Synthetic polymers could amplify the outer coordination sphere effect since tens and hundreds of functional groups can be added in polymers. The presence of those functional groups on polymers changes the chemical environment of metals, leading to an improvement in the catalytic efficiency. McCrory and coworkers demonstrated that poly(4-vinylpyridine) (P4VP) possibly as a weak base could control the localized proton concentration around metal sites (Fig. 10b).[215] They used cobalt phthalocyanine (CoPc) as an electrocatalyst for CO_2 electroreduction with P4VP. CoPc–P4VP showed a selectivity of 89 ± 3% to produce CO, while the selectivity for CO_2 to CO was 36 ± 7% for CoPc solely. The weakly protonated P4VP under pH 4.7 could deliver enough protons to carry out proton-assisted electroreduction of CO_2 while preventing proton reduction.[229]

A few groups reported the outer coordination sphere effect provided by polymeric bases to improve the activity for proton reduction.[32,228,230,231] Hydrogenase as one type of anaerobic enzymes reduces protons to hydrogen. The [2Fe–2S] cluster with a $(\mu\text{-}S_2)Fe_2(CO)_6$ structure can mimic the diiron active sites in hydrogenases. Incorporating the [2Fe–2S] cluster in water-soluble polymers can increase the solubility and stability of the cluster. Pyun and coworkers designed polymer-grafted [2Fe–2S] using atom transfer radical polymerization (Fig. 11a).[228] Starting with a Br symmetrical initiator prepared from [2Fe–2S] hydroquinone reacting with a-bromoisobutyryl bromide, methacrylate-based monomers could grow on the [2Fe–2S] cluster. The cluster grafted with poly(2-dimethylamino)ethyl methacrylate (PDMAEMA) was extremely active to reduce protons with a high current density of $J = 22$ mA cm^{-2} at the reduction peak. According to the results from the Tafel plots, a lower overpotential (0.2 V) compared to that of a Pt disk could be achieved to reach a turnover of 25 000 s^{-1}. The high activity was a result of protonated PDMAEMA at pH 7 enhancing the localized proton concentration. When grafting with non-ionic polymers, e.g., poly(oligo(ethylene glycol)methyl ether methacrylate) (POEGMA), the [2Fe–2S] cluster was inactive to produce hydrogen (Fig. 11b).[217]

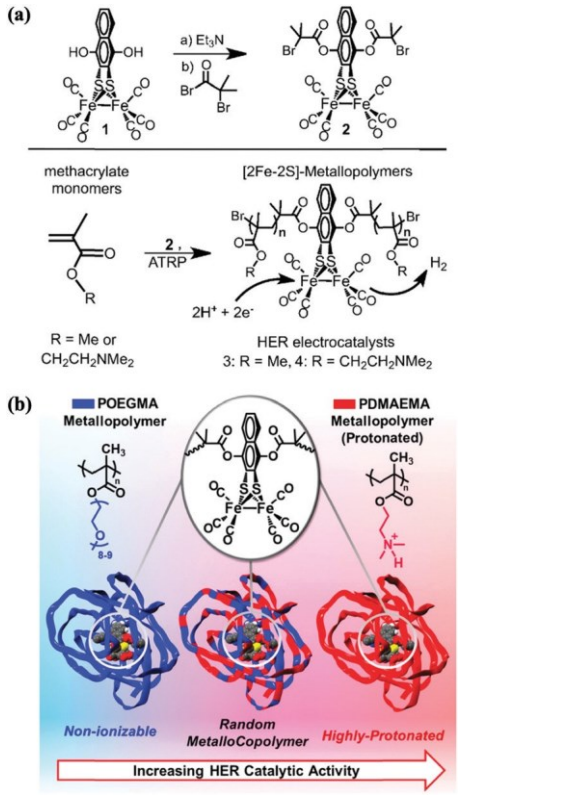

Fig. 11 (a) Synthesis of the [2Fe–2S]-containing initiator and the chemical structure of corresponding poly(methacrylate). (b) Comparison of [2Fe–2S]-containing polymers and hydrogenases for hydrogen production. Figure (a) reproduced from ref. 228, copyright 2018 Wiley VCH; [228] figure (b) reproduced from ref. 217, copyright 2018 American Chemical Society.[217]

5.2 Metal-containing single chain nanoparticles (SCNPs)

While linear polymers can improve the catalytic efficiency of metal ions, the resultant activity of metal ions is still far from that of metalloenzymes. To create more sophisticated outer coordination environments of metal sites, there have been numerous efforts in metal-containing SCNPs. SCNPs are self-collapsed random coils and their sizes are in the range of 5–40 nm, fairly close to that of metalloenzymes. Many intramolecular cross-linking chemistries have been developed in the past, such as covalent coupling, hydrogen bonding, hydrophobic interactions and M–L coordination. Interested readers can find more details in recent review articles.[232–235] When confining metal sites in SCNPs, there is a higher degree of controllability of the outer coordination sphere that is not possible for linear polymers.[236] Other than the advantages of linear polymers, SCNPs can provide hydrophobic or chiral domains even in water-rich solvents, and SCNPs can possibly confine two or more types of metals for cascade reactions.

Catalytically active metals can be incorporated in SCNPs using M–L coordination as non-covalent cross-linking. Pomposo and coworkers designed Cu^{2+}-containing SCNPs using a copolymer of methyl methacrylate (MMA) and 2-(acetoacetoxy)ethyl methacrylate (AEMA) (Fig. 12a).[237] Cu^{2+} ions bound with two b-ketoesters triggered the self-collapse of the polymer chains. The size of the Cu^{2+}-containing SCNPs was around 15 nm. Those hybrid catalysts were very active and highly selective to catalyze the oxidative coupling reaction of acetylenes. Even at a low catalyst loading of B0.5 mol% at which $Cu(OAc)_2$ and $Cu(acac)_2$ were inactive, the Cu^{2+}-containing SCNPs were highly active (4-98% yield) for the coupling of propargyl acetate. Interestingly, the Cu^{2+}-containing SCNPs were very selective to propargyl substrates with different molecular sizes. Using a mixture of substrates including propargyl acetate, propargyl benzoate and octyne, the Cu^{2+}-containing SCNPs only catalyzed the homocoupling of propargyl acetate. Again, such selectivity did not exist in $Cu(OAc)_2$ nor $Cu(acac)_2$. The local environment, particular loosely compacted polymer chains around the catalytic sites, limited the access of more bulky substrates. A follow up work from Pomposo et al. demonstrated that Cu^{2+}-containing SCNPs catalyzed water-phase radical polymerization.[238] The Cu^{2+}-containing SCNPs as compared to laccase showed much better thermostability. Cu^{2+}-Containing SCNPs can catalyze many other reactions, like alkyne-azide click reactions and epoxidation of C=C bonds. Zimmerman and coworkers showed that Cu^{2+}-containing SCNPs with low toxicity even catalyzed alkyne–azide click reactions within live cells.[239]

Other than Cu^{2+} ions, Pt^{2+},[242] Pd^{2+},[240,243] Ru^{2+},[244] Rh^{+},[245] Ir^{+},[246] and Ti^{4+} (ref. 247) have been studied in SCNPs as catalysts for various reactions. Knofel et al. designed Pt^{2+}-containing polystyrene SCNPs using triphenylphosphine as a ligand.[248] With phosphine ligands, it is possible to study the coordination in solution using ^{31}P NMR spectroscopy. Interestingly, they found that triphenylphosphine was all bound to Pt^{2+} ions in two different configurations. Pt^{2+}-Containing polystyrene SCNPs were as active as monomeric complex cis-$Pt(PPh_3)_2Cl_2$ for amination of allyl alcohol but recyclable and reusable through simple dialysis. Zhang et al. synthesized Ti^{4+}-containing SCNPs using chiral salen ligands in water-soluble PNIPAM.[247] Those Ti^{4+}-containing SCNPs were active for an asymmetric sulfoxdiation reaction with high activity (conversion, 85–99%) within 1 h and the enantioselectivity reached 95–98%.[247] The catalytic efficiency was greatly improved when increasing the hydrophobicity of the substrates and retaining high enantioselectivity. Those catalysts were also recyclable up to 8 times by simply using the LCST transition of PNIPAM.[249] Lemcoff and coworkers reported the preparation of p-bound metal-containing SCNPs from polyolefins.[250,251] Instead of polymerizing complicated ligands, they used ring-opening polymerization to synthesize poly(1,5-cyclooctadiene) with 1,5-diene repeating units. The presence of p bonds could coordinate Rh^{+} and Ir^{+} through ligand exchange. Using the cross coupling of phenyl boronic acid and 4-nitrobenzaldehyde as an example, Rh^{+}-containing SCNPs showed moderate activity but unique selectivity to homo-coupling to form biphenyl (4-99%). N-heterocyclic carbenes (NHCs) are a strong ligand for a variety of metals through metal–C bonds. NHCs also show interesting s donation to transition metals to stabilize metals in the air and promote their reactivity. Lambert et al. designed Pd^{2+}-containing SCNPs from a copolymer of water-soluble PEG-grafted PS and 4-vinylbenzylethylbenzimidazolium chloride (Fig. 12b). Pd^{2+} bound with benzimidazolium to form Pd^{2+}–NHC coordination, resulting in the formation of SCNPs with a

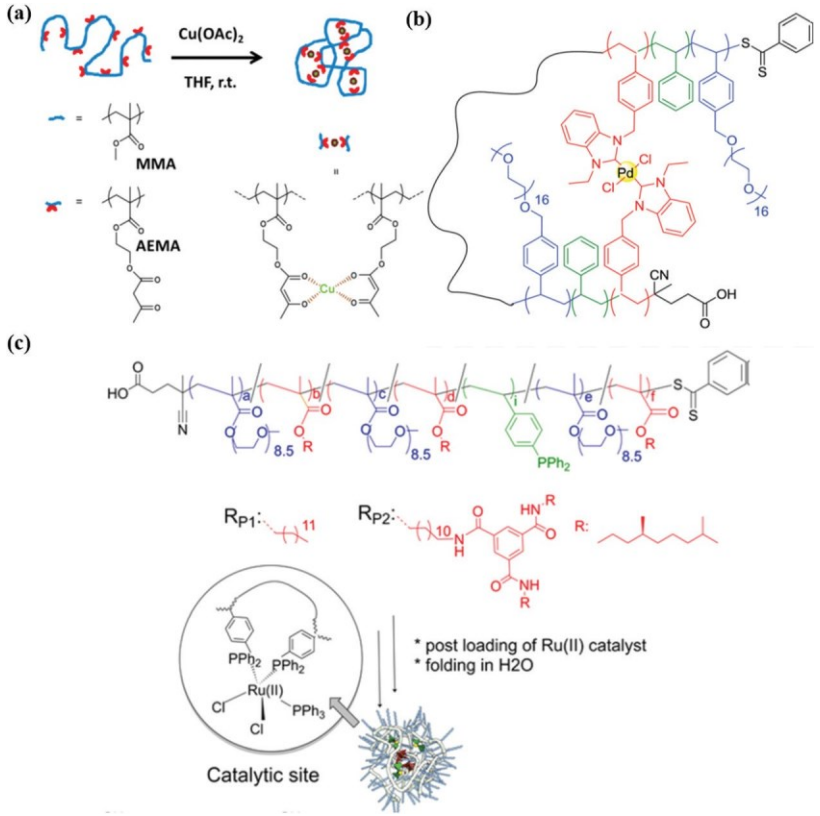

Fig. 12 (a) Chemical structure of Cu^{2+}-containing SCNPs. (b) PEG-b-PS SCNPs formed with Pd–NHC coordination. (c) Chemical structure of Ru^{2+}-containing SCNPs driven by BTA intramolecular crosslinking and SCNPs containing phosphine–Pt^{2+}. Figure (a) reproduced from ref. 237, copyright 2014 American Chemical Society;[237] figure (b) reproduced from ref. 240, copyright 2018 The Royal Society of Chemistry;[240] figure (c) reproduced from ref. 241, copyright 2015 American Chemical Society.[241]

hydrodynamic diameter of 9.7 nm. Pd^{2+}–NHC in SCNPs was very active for the Suzuki coupling reaction of 4-iodotoluene and phenyl boronic acid. The SCNPs showed 100% conversion within 5 h, while that of the molecular benchmark $Pd(OAc)_2$ was 24 h.[240]

Control of the localized coordination environments of metal sites is the key to improving their reactivity. For example, natural metalloenzymes have the catalytic metal(s) confined in hydrophobic pockets around folded proteins. One can mimic such hydrophobic pockets in similar hydrophobic domains in metal-containing SCNPs.[252,253] The studies from Meijer and Palmans have extensively addressed the challenges in controlling the localized coordination environments of metal sites, including hydrophobic pockets and chiral structures. The benzene-1,3,5-tricarboxamide (BTA) moieties often used for control over the folding structures of SCNPs can stack 1-D helically through three hydrogen bonds.[254] Using BTAs in water soluble copolymers, a family of SCNPs with hydrophobic pockets has been designed.[255–264] The formation of those supramolecular structures through multiple hydrogen bonds was found to be essential for catalysis. For example, in L-proline-containing SCNPs, only SCNPs with the structuring element formed by BTA stacking were active for aldol reactions of p-nitrobenzaldehyde and cyclohexaneone.[265] Those hydrophobic domains possibly isolated L-proline (catalytic sites) from the bulk medium. Together with the improvement of the local concentration of the substrates around active sites, the hydrophobic interaction was the key to receive high activity. With triphenylphosphine ligands, Ru^{2+}-containing SCNPs prepared in a similar fashion were active for hydrogenation of cyclohexanone and oxidation of secondary alcohols in water (Fig. 12c).[241] The presence of hydrophobic domains had a profound impact on the selectivity. For the oxidation of secondary alcohols, when a cocktail mixture of cyclohexanol, 4-tetrahydropyranol and 4-tert-butylcyclohexanol was examined in acetone, the Ru^{2+}-containing SCNPs showed nearly identical reactivity for all three alcohols. In contrast, the reactivity of the Ru^{2+}-containing SCNPs was significantly different when the oxidation was carried out in water. A faster turnover toward the oxidation of 4-tert-butylcyclohexanol was seen among the three substrates. The hydrophobic domains in the SCNPs therefore provided proximity to certain substrates that were favorable to access the metal site. With DPA and phenanthroline, Cu^{2+}-containing SCNPs were designed for the click reactions of azides and alkynes. There was a dramatic enhancement in reactivity when incorporating Cu^{2+} ions in SCNPs.

One of the advantages of using metal-containing SCNPs is to enhance the stability of metal catalysts in water. When confined within collapsed polymer chains, the biological toxicity of metal ions can be reduced. Although their catalytic efficiency is still too low compared to that of metalloenzymes, it is possible to use metal-containing SCNPs to catalyze reactions in living systems as a ''true'' synthetic enzyme. Palmans and coworkers

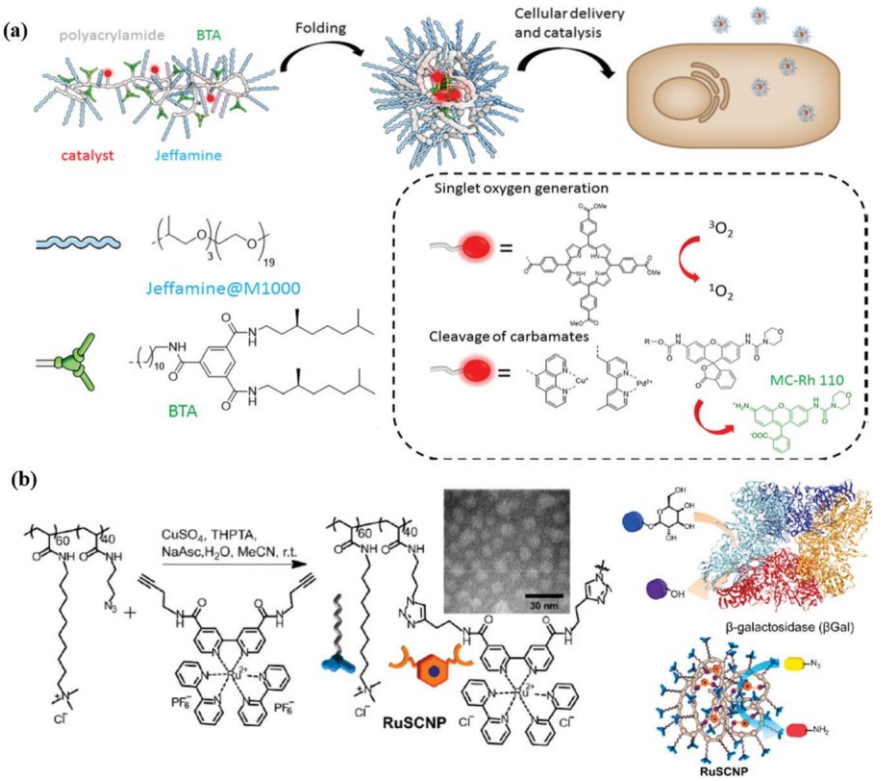

Fig. 13 (a) Scheme illustrating the folding of SCNPs and the catalysis in enzymes and the corresponding chemical structures.[266] (b) Chemical structure of Ru^{2+}-containing SCNPs and concept of dual catalysis in enzymes.[31] Figure (a) reproduced from ref. 266, copyright 2018 American Chemical Society, DOI: 10.1021/jacs.8b00122;[266] figure (b) reproduced from ref. 31, copyright 2020 American Chemical Society.[31]

used BTA-containing SCNPs to catalyze a catalytic cleavage of rhodamine-based fluorophores (Fig. 13a).[266] When coordinated with Cu^{+} and Pd^{2+} ions, those SCNPs catalyzed carbamate cleavage reactions for fluorophores both in solution and in cellar media. There was little impact of the HeLa cells on the catalytic carbamate cleavage reactions. More recently, Zimmerman's group designed an intracellular catalysis system using Ru^{2+}-containing SCNPs (Fig. 13b).[31] Ru^{2+}-Containing SCNPs could catalyze photochemical reduction of azide-containg fluorogenic rhodamine 110, which was fluorescent after reduction. Ru^{2+}-Containing SCNPs could further bond with another enzyme (2–3 SCNPs per enzyme on average), b-galactosidase (bGal), which catalyzes the b-galactoside hydrolysis reaction. The SCNP–bGal conjugates were able to catalyze a tandem reaction intracellularly. A complex fluorogenic molecule, azido phenyl carbonate b-galacto coumarin, was used for this purpose. The Ru^{2+}-containing SCNPs first catalyzed the photo-reduction of azido and then the cleavage of phenyl carbonate to expose b-galacto coumarin. Subsequently, b-galacto coumarin underwent hydrolysis to turn on the fluorescence of coumarin. 20% conversion was reached after 10 min within HeLa cells. Those results are remarkable and potentially bridge the gap between synthetic and natural enzymes in bio-related catalysis.

6. Summary and outlook

We have reviewed the recent advances in metal/polymer hybridization through non-covalent M–L coordination to design multifunctional materials. Coordinating metal ions with synthetic polymers provides a valuable strategy to control the synergetic outcomes such as the optical, mechanical and catalytic functionalities of hybrids. On one hand, the built-in non-covalent networks through the dynamic M–L coordination enable self-healing and recoverable toughness in elastic polymers. The coordination strength enables the precise control of the self-healing efficiency and the recovery proficiency of toughness. On the other hand, synthetic polymers endow stimuli-responsiveness to metals and provide positive catalytic enhancement to metal sites. With luminescent metals, coupling synthetic polymers with metals enables adaptive behaviors of hybrids, i.e., varying the luminescence emission of hybrids in response to a change in the environment. With catalytically active metals, synthetic polymers offer secondary coordination environments to metals, which opens up new opportunities to design bioinspired catalysts as synthetic mimics of metalloenzymes.

Although loading metals on synthetic polymers is not new, there are many more functionalities and new synergies through hybridization yet to be discovered. In the light of bioinspired catalysis, metal/polymer hybrids still have plenty of room to improve and explore. The current knowledge is only limited to a few model reactions using hybrid catalysts with one type of metal sites. As for enzymatic catalysis, it is common to see cooperativity among a number of enzymes to convert substrates in a convergent cascade. Previous studies from Finn et al. suggested the rolling mechanism between dendritic catalysts

and dendritic substrates.[219] Rolling instead of diffusing can enhance the reaction kinetics by three magnitudes. It is, therefore, convincing that integrating multiple catalytic sites on synthetic polymers possibly improves the catalytic efficiency of consecutive reactions, if those catalytic sites are encodable in sequence as well. How to encode multiple catalytic metals in polymers, particular facing the challenges of dynamic coordination, has not been realized yet, although there are some examples in supramolecules.[267] Additionally, more sophisticated cooperativity, e.g., with enzymes and nanocatalysts, can be coupled in those hybrid catalysts as demonstrated by Zimmerman et al.[31]

There has been rising attention in switchable materials that have multiple mechanical states in response to external stimuli. M–L coordination has lots of potential in the design of those switchable materials. As discussed earlier in Sections 2 and 3, the coordination is stimuli-responsive, e.g., a nearly universal response to pH changes in pyridine-containing ligands. In lanthanide complexes, moisture can disrupt the Ln–N coordination. Recent examples also show the response of the M–L coordination to light, as a more robust and spatial/temporal controllable stimulus. In the example reported by Wu et al., the two coordination states of Ru^{2+}–thioether and Ru^{2+}–H_2O are light-switchable to control the network strength.[268] The other example from Johnson et al. also suggests that Pd^{2+} complexes with bis-pyridyl dithienylethene are light-switchable to control the network topology and the mechanical strength of polymer/metal hybrids.[269] The new development of this adaptive M–L binding can further lead to the design of light-activated actuators and soft robotics. Moreover, all those changes in mechanical states can be coupled with optical properties of metals in the form of absorption and luminescence. It will also be possible to use simple optical tools as a readout of the mechanical strength of those materials.

Conflicts of interest

There are no conflicts to declare.

Acknowledgements

J. H. is grateful for the continuous financial support from the University of Connecticut, the Green Emulsions, Micelles and Surfactants (GEMS) Center, ACS petroleum research foundation, and the National Science Foundation (CBET-1705566). G. W. is grateful for the financial support of Zhejiang Provincial Natural Science Foundation of China (grant no. LY19E030002) and Ningbo Municipal Science and Technology Bureau (grant no. 2019A610133).

Notes and references

1 F. M. Winnik, Macromolecules, 1990, 23, 233–242.
2 N. A. Platé, T. L. Lebedeva and L. I. Valuev, Polym. J., 1999, 31, 21–27.
3 X. Zhu, D. Avoce, H. Liu and A. Benrebouh, Macromol. Symp., 2004, 1, 187–192.
4 A. Lendlein and R. S. Trask, Multifunct. Mater., 2018, 1, 010201.
5 A. Juris, V. Balzani, F. Barigelletti, S. Campagna, P. Belser and A. von Zelewsky, Coord. Chem. Rev., 1988, 84, 85–277.
6 M. J. MacLachlan, M. Ginzburg, N. Coombs, T. W. Coyle, N. P. Raju, J. E. Greedan, G. A. Ozin and I. Manners, Science, 2000, 287, 1460–1463.
7 Y. Sun and Y. Xia, Analyst, 2003, 128, 686–691.
8 N. E. Leadbeater and M. Marco, Chem. Rev., 2002, 102, 3217–3274.
9 Y. Li, M. Beija, S. Laurent, L. v. Elst, R. N. Muller, H. T. Duong, A. B. Lowe, T. P. Davis and C. Boyer, Macromolecules, 2012, 45, 4196–4204.
10 H. Yersin and W. J. Finkenzeller, Highly Efficient OLEDs with Phosphorescent Materials, 2008, pp. 1–97.
11 Z. Nie, D. Fava, E. Kumacheva, S. Zou, G. C. Walker and M. Rubinstein, Nat. Mater., 2007, 6, 609–614.
12 J. He, X. Huang, Y.-C. Li, Y. Liu, T. Babu, M. A. Aronova, S. Wang, Z. Lu, X. Chen and Z. Nie, J. Am. Chem. Soc., 2013, 135, 7974–7984.
13 C. Yi, Y. Yang, B. Liu, J. He and Z. Nie, Chem. Soc. Rev., 2020, 49, 465–508.
14 L. Liu, R. Aleisa, Y. Zhang, J. Feng, Y. Zheng, Y. Yin and W. Wang, Angew. Chem., Int. Ed., 2019, 131, 16453–16459.
15 N. Zou, G. Chen, X. Mao, H. Shen, E. Choudhary, X. Zhou and P. Chen, ACS Nano, 2018, 12, 5570–5579.
16 G. Chen, Y. Wang, M. Yang, J. Xu, S. J. Goh, M. Pan and H. Chen, J. Am. Chem. Soc., 2010, 132, 3644–3645.
17 G. E. Oosterom, J. N. Reek, P. C. Kamer and P. W. van Leeuwen, Angew. Chem., Int. Ed., 2001, 40, 1828–1849.
18 K. Liu, N. Zhao and E. Kumacheva, Chem. Soc. Rev., 2011, 40, 656–671.
19 P. Yin, D. Li and T. Liu, Chem. Soc. Rev., 2012, 41, 7368–7383.
20 C. Yi, S. Zhang, K. T. Webb and Z. Nie, Acc. Chem. Res., 2017, 50, 12–21.
21 B. Gao, M. J. Rozin and A. R. Tao, Nanoscale, 2013, 5, 5677–5691.
22 P. Chen, Q. Li, S. Grindy and N. Holten-Andersen, J. Am. Chem. Soc., 2015, 137, 11590–11593.
23 G. Weng, S. Thanneeru and J. He, Adv. Mater., 2018, 30, 1706526.
24 X. Zhou, L. Wang, Z. Wei, G. Weng and J. He, Adv. Funct. Mater., 2019, 29, 1903543.
25 Q. Zhu, K. Van Vliet, N. Holten-Andersen and A. Miserez, Adv. Funct. Mater., 2019, 29, 1808191.
26 L. Shi, H. Carstensen, K. Hölzl, M. Lunzer, H. Li, J. Hilborn, A. Ovsianikov and D. A. Ossipov, Chem. Mater., 2017, 29, 5816–5823.
27 N. Holten-Andersen, M. J. Harrington, H. Birkedal, B. P. Lee, P. B. Messersmith, K. Y. C. Lee and J. H. Waite, Proc. Natl. Acad. Sci. U. S. A., 2011, 108, 2651–2655.
28 X. Cui, Y. Song, J.-P. Wang, J.-K. Wang, Q. Zhou, T. Qi and G. L. Li, Polymer, 2019, 174, 143–149.
29 J. Suriboot, C. E. Hobbs, W. Guzman, H. S. Bazzi and D. E. Bergbreiter, Macromolecules, 2015, 48, 5511–5516.
30 Y. Niu, L. K. Yeung and R. M. Crooks, J. Am. Chem. Soc., 2001, 123, 6840–6846.

31 J. Chen, K. Li, J. S. L. Shon and S. C. Zimmerman, J. Am. Chem. Soc., 2020, 142, 4565–4569.
32 W. P. Brezinski, M. Karayilan, K. E. Clary, N. G. Pavlopoulos, S. Li, L. Fu, K. Matyjaszewski, D. H. Evans, R. S. Glass and D. L. Lichtenberger, Angew. Chem., Int. Ed., 2018, 57, 11898–11902.
33 C. S. K. Mak and W. K. Chan, Highly efficient OLEDs with phosphorescent materials, 2008, pp. 329–362.
34 Y. Yan, J. Zhang, L. Ren and C. Tang, Chem. Soc. Rev., 2016, 45, 5232–5263.
35 S. V. Eliseeva and J.-C. G. Bünzli, Chem. Soc. Rev., 2010, 39, 189–227.
36 A. de Bettencourt-Dias, Luminescence of lanthanide ions in coordination compounds and nanomaterials, John Wiley & Sons, 2014.
37 J. B. Beck and S. J. Rowan, J. Am. Chem. Soc., 2003, 125, 13922–13923.
38 H. S. Jung, P. S. Kwon, J. W. Lee, J. I. Kim, C. S. Hong, J. W. Kim, S. Yan, J. Y. Lee, J. H. Lee and T. Joo, J. Am. Chem. Soc., 2009, 131, 2008–2012.
39 J. Maiti, B. Pokhrel, R. Boruah and S. K. Dolui, Sens. Actuators, B, 2009, 141, 447–451.
40 S. C. Yu, X. Gong and W. K. Chan, Macromolecules, 1998, 31, 5639–5646.
41 S. C. Yu, S. Hou and W. K. Chan, Macromolecules, 1999, 32, 5251–5256.
42 S. C. Yu, S. Hou and W. K. Chan, Macromolecules, 2000, 33, 3259–3273.
43 W. Y. Ng, X. Gong and W. K. Chan, Chem. Mater., 1999, 11, 1165–1170.
44 J. R. Kumpfer and S. J. Rowan, J. Am. Chem. Soc., 2011, 133, 12866–12874.
45 Z. Wei, S. Thanneeru, E. Margaret Rodriguez, G. Weng and J. He, Soft Matter, 2020, 16, 2276–2284.
46 A. Heller, J. Am. Chem. Soc., 1966, 88, 2058–2059.
47 Y. Haas and G. Stein, J. Phys. Chem., 1971, 75, 3668–3677.
48 J. Chrysochoos, Spectrosc. Lett., 1972, 5, 57–67.
49 S. J. Rowan and J. B. Beck, Faraday Discuss., 2005, 128, 43–53.
50 S.-G. Liu, J.-L. Zuo, Y.-Z. Li and X.-Z. You, J. Mol. Struct., 2004, 705, 153–157.
51 W. Weng, J. B. Beck, A. M. Jamieson and S. J. Rowan, J. Am. Chem. Soc., 2006, 128, 11663–11672.
52 R. Shunmugam and G. N. Tew, J. Am. Chem. Soc., 2005, 127, 13567–13572.
53 Q. Zhang, S. Niu, L. Wang, J. Lopez, S. Chen, Y. Cai, R. Du, Y. Liu, J. C. Lai and L. Liu, Adv. Mater., 2018, 30, 1801435.
54 Z. Wang, C. Xie, C. Yu, G. Fei, Z. Wang and H. Xia, Macromol. Rapid Commun., 2018, 39, 1700678.
55 C. Hu, M. X. Wang, L. Sun, J. H. Yang, M. Zrínyi and Y. M. Chen, Macromol. Rapid Commun., 2017, 38, 1600788.
56 S. Liu, J. Ling, K. Li, F. Yao, O. Oderinde, Z. Zhang and G. Fu, Compos. Sci. Technol., 2017, 145, 62–70.
57 Q.-F. Li, S. Chu, E. Li, M. Li, J.-T. Wang and Z. Wang, Dyes Pigm., 2020, 174, 108091.
58 D. W. Balkenende, S. Coulibaly, S. Balog, Y. C. Simon, G. L. Fiore and C. Weder, J. Am. Chem. Soc., 2014, 136, 10493–10498.
59 R. B. Martin and J. A. Lissfelt, J. Am. Chem. Soc., 1956, 78, 938–940.
60 R. Shunmugam and G. N. Tew, Polym. Adv. Technol., 2007, 18, 940–945.
61 R. Shunmugam and G. N. Tew, Polym. Adv. Technol., 2008, 19, 596–601.
62 J. Yuan, X. Fang, L. Zhang, G. Hong, Y. Lin, Q. Zheng, Y. Xu, Y. Ruan, W. Weng and H. Xia, J. Mater. Chem., 2012, 22, 11515–11522.
63 Z. Zhou, Z. Wang, Y. Tang, Y. Zheng and Q. Wang, J. Mater. Sci., 2019, 54, 2526–2534.
64 Q. Zhu, L. Zhang, K. Van Vliet, A. Miserez and N. Holten-Andersen, ACS Appl. Mater. Interfaces, 2018, 10, 10409–10418.
65 C. Yang, J. Xu, R. Zhang, Y. Zhang, Z. Li, Y. Li, L. Liang and M. Lu, Sens. Actuators, B, 2013, 177, 437–444.
66 A. Balamurugan, M. Reddy and M. Jayakannan, J. Mater. Chem. A, 2013, 1, 2256–2266.
67 Y. Yao, Y. Wang, Z. Li and H. Li, Langmuir, 2015, 31, 12736–12741.
68 K. Meng, C. Yao, Q. Ma, Z. Xue, Y. Du, W. Liu and D. Yang, Adv. Sci., 2019, 6, 1802112.
69 B. Yang, H. Zhang, H. Peng, Y. Xu, B. Wu, W. Weng and L. Li, Polym. Chem., 2014, 5, 1945–1953.
70 Y. Yamamoto, S. Sawa, Y. Funada, T. Morimoto, M. Falkenström, H. Miyasaka, S. Shishido, T. Ozeki, K. Koike and O. Ishitani, J. Am. Chem. Soc., 2008, 130, 14659–14674.
71 A. K. Saha, K. Kross, E. D. Kloszewski, D. A. Upson, J. L. Toner, R. A. Snow, C. D. V. Black and V. C. Desai, J. Am. Chem. Soc., 1993, 115, 11032–11033.
72 M. Yao and W. Chen, Anal. Chem., 2011, 83, 1879–1882.
73 F. Fueyo-González, E. Garcia-Fernandez, D. Martínez, L. Infantes, A. Orte, J. A. González-Vera and R. Herranz, Chem. Commun., 2020, 56, 5484–5487.
74 L. Natrajan, J. Pécaut, M. Mazzanti and C. LeBrun, Inorg. Chem., 2005, 44, 4756–4765.
75 A. M. Nonat, A. J. Harte, K. Sénéchal-David, J. P. Leonard and T. Gunnlaugsson, Dalton Trans., 2009, 4703–4711.
76 E. M. Surender, S. J. Bradberry, S. A. Bright, C. P. McCoy, D. C. Williams and T. Gunnlaugsson, J. Am. Chem. Soc., 2017, 139, 381–388.
77 C. P. McCoy, F. Stomeo, S. E. Plush and T. Gunnlaugsson, Chem. Mater., 2006, 18, 4336–4343.
78 Q.-F. Li, X. Du, L. Jin, M. Hou, Z. Wang and J. Hao, J. Mater. Chem. C, 2016, 4, 3195–3201.
79 S. J. Bradberry, G. Dee, O. Kotova, C. P. McCoy and T. Gunnlaugsson, Chem. Commun., 2019, 55, 1754–1757.
80 G. Anderegg, F. Arnaud-Neu, R. Delgado, J. Felcman and K. Popov, Pure Appl. Chem., 2005, 77, 1445–1495.
81 T. Singha Mahapatra, H. Singh, A. Maity, A. Dey, S. K. Pramanik, E. Suresh and A. Das, J. Mater. Chem. C, 2018, 6, 9756–9766.
82 L. Shi, P. Ding, Y. Wang, Y. Zhang, D. Ossipov and J. Hilborn, Macromol. Rapid Commun., 2019, 40, 1800837.
83 H. Tan, Q. Li, C. Ma, Y. Song, F. Xu, S. Chen and L. Wang, Biosens. Bioelectron., 2015, 63, 566–571.
84 H. Chen, Y. Xie, A. M. Kirillov, L. Liu, M. Yu, W. Liu and Y. Tang, Chem. Commun., 2015, 51, 5036–5039.

85 Y. Song, J. Chen, D. Hu, F. Liu, P. Li, H. Li, S. Chen, H. Tan and L. Wang, Sens. Actuators, B, 2015, 221, 586–592.
86 M. Xu, Z. Gao, Q. Zhou, Y. Lin, M. Lu and D. Tang, Biosens. Bioelectron., 2016, 86, 978–984.
87 Y. Liu, S. Zhou, L. Fan and H. Fan, Microchim. Acta, 2016, 183, 2605–2613.
88 M. D. Yilmaz and H. A. Oktem, Anal. Chem., 2018, 90, 4221–4225.
89 Z. Zhou, J. Gu, X. Qiao, H. Wu, H. Fu, L. Wang, H. Li and L. Ma, Sens. Actuators, B, 2019, 282, 437–442.
90 L. Fabbrizzi, M. Licchelli, P. Pallavicini, D. Sacchi and A. Taglietti, Analyst, 1996, 121, 1763–1768.
91 B. Valeur and I. Leray, Coord. Chem. Rev., 2000, 205, 3–40.
92 L. Prodi, F. Bolletta, M. Montalti and N. Zaccheroni, Coord. Chem. Rev., 2000, 205, 59–83.
93 Y. Mei, P. A. Bentley and W. Wang, Tetrahedron Lett., 2006, 47, 2447–2449.
94 H. Yersin, A. F. Rausch, R. Czerwieniec, T. Hofbeck and T. Fischer, Coord. Chem. Rev., 2011, 255, 2622–2652.
95 S. W. Thomas, G. D. Joly and T. M. Swager, Chem. Rev., 2007, 107, 1339–1386.
96 X.-Y. Chen, X. Yang and B. J. Holliday, J. Am. Chem. Soc., 2008, 130, 1546–1547.
97 P. T. Furuta, L. Deng, S. Garon, M. E. Thompson and J. M. Fréchet, J. Am. Chem. Soc., 2004, 126, 15388–15389.
98 M. A. Baldo, D. F. O'Brien, M. E. Thompson and S. R. Forrest, Phys. Rev. B: Condens. Matter Mater. Phys., 1999, 60, 14422–14428.
99 S. Lamansky, P. Djurovich, D. Murphy, F. Abdel-Razzaq, H.-E. Lee, C. Adachi, P. E. Burrows, S. R. Forrest and M. E. Thompson, J. Am. Chem. Soc., 2001, 123, 4304–4312.
100 M. A. Rawashdeh-Omary, J. M. Lopez-de-Luzuriaga, M. D. Rashdan, O. Elbjeirami, M. Monge, M. Rodriguez-Castillo and A. Laguna, J. Am. Chem. Soc., 2009, 131, 3824–3825.
101 J. Wang, Q. He, C. Wang and W. Bu, Soft Matter, 2018, 14, 31–34.
102 S. Y. An, D. Arunbabu, S. M. Noh, Y. K. Song and J. K. Oh, Chem. Commun., 2015, 51, 13058–13070.
103 S. Burattini, B. W. Greenland, D. Chappell, H. M. Colquhoun and W. Hayes, Chem. Soc. Rev., 2010, 39, 1973–1985.
104 Z. Wei, J. H. Yang, J. Zhou, F. Xu, M. Zrínyi, P. H. Dussault, Y. Osada and Y. M. Chen, Chem. Soc. Rev., 2014, 43, 8114–8131.
105 F. Herbst, D. Döhler, P. Michael and W. H. Binder, Macromol. Rapid Commun., 2013, 34, 203–220.
106 M. A. Tasdelen, Polym. Chem., 2011, 2, 2133–2145.
107 G. M. Scheutz, J. J. Lessard, M. B. Sims and B. S. Sumerlin, J. Am. Chem. Soc., 2019, 141, 16181–16196.
108 Y. Chen and Z. Guan, Chem. Commun., 2014, 50, 10868–10870.
109 Y. Chen, A. M. Kushner, G. A. Williams and Z. Guan, Nat. Chem., 2012, 4, 467.
110 S. Burattini, H. M. Colquhoun, J. D. Fox, D. Friedmann, B. W. Greenland, P. J. Harris, W. Hayes, M. E. Mackay and S. J. Rowan, Chem. Commun., 2009, 6717–6719.
111 G. Jiang, C. Liu, X. Liu, G. Zhang, M. Yang, Q. Chen and F. Liu, J. Macromol. Sci., Part A: Pure Appl. Chem., 2010, 47, 335–342.
112 D. C. Tuncaboylu, M. Sari, W. Oppermann and O. Okay, Macromolecules, 2011, 44, 4997–5005.
113 D. C. Tuncaboylu, A. Argun, M. Sahin, M. Sari and O. Okay, Polymer, 2012, 53, 5513–5522.
114 Y.-L. Rao, A. Chortos, R. Pfattner, F. Lissel, Y.-C. Chiu, V. Feig, J. Xu, T. Kurosawa, X. Gu and C. Wang, J. Am. Chem. Soc., 2016, 138, 6020–6027.
115 Y. Shi, M. Wang, C. Ma, Y. Wang, X. Li and G. Yu, Nano Lett., 2015, 15, 6276–6281.
116 Y.-L. Rao, A. Chortos, R. Pfattner, F. Lissel, Y.-C. Chiu, V. Feig, J. Xu, T. Kurosawa, X. Gu, C. Wang, M. He, J. W. Chung and Z. Bao, J. Am. Chem. Soc., 2016, 138, 6020–6027.
117 Z. Wei, J. He, T. Liang, H. Oh, J. Athas, Z. Tong, C. Wang and Z. Nie, Polym. Chem., 2013, 4, 4601–4605.
118 H. Lee, N. F. Scherer and P. B. Messersmith, Proc. Natl. Acad. Sci. U. S. A., 2006, 103, 12999–13003.
119 Q. Li, D. G. Barrett, P. B. Messersmith and N. Holten-Andersen, ACS Nano, 2016, 10, 1317–1324.
120 M. S. Menyo, C. J. Hawker and J. H. Waite, Soft Matter, 2013, 9, 10314–10323.
121 J. K. Hirschberg, L. Brunsveld, A. Ramzi, J. A. Vekemans, R. P. Sijbesma and E. Meijer, Nature, 2000, 407, 167–170.
122 H. E. Bryndza, L. K. Fong, R. A. Paciello, W. Tam and J. E. Bercaw, J. Am. Chem. Soc., 1987, 109, 1444–1456.
123 A. Avdeef, S. R. Sofen, T. L. Bregante and K. N. Raymond, J. Am. Chem. Soc., 1978, 100, 5362–5370.
124 M. Zhong, R. Wang, K. Kawamoto, B. D. Olsen and J. A. Johnson, Science, 2016, 353, 1264–1268.
125 S. V. Wegner, F. C. Schenk, S. Witzel, F. Bialas and J. P. Spatz, Macromolecules, 2016, 49, 4229–4235.
126 F. Peng, G. Li, X. Liu, S. Wu and Z. Tong, J. Am. Chem. Soc., 2008, 130, 16166–16167.
127 W. Sun, S. Li, B. Häupler, J. Liu, S. Jin, W. Steffen, U. S. Schubert, H. J. Butt, X. J. Liang and S. Wu, Adv. Mater., 2017, 29, 1603702.
128 W. Sun, M. Parowatkin, W. Steffen, H. J. Butt, V. Mailänder and S. Wu, Adv. Healthcare Mater., 2016, 5, 467–473.
129 X. Xu, Q. Zhang, K. Liu, N. Liu, Y. Han, W. Chen, C. Xie, P. Li and J. He, Polym. Chem., 2019, 10, 3585–3596.
130 S. W. Taylor, D. B. Chase, M. H. Emptage, M. J. Nelson and J. H. Waite, Inorg. Chem., 1996, 35, 7572–7577.
131 N. Holten-Andersen, G. E. Fantner, S. Hohlbauch, J. H. Waite and F. W. Zok, Nat. Mater., 2007, 6, 669–672.
132 F. Peng, G. Li, X. Liu, S. Wu and Z. Tong, J. Am. Chem. Soc., 2008, 130, 16166–16167.
133 M. J. Harrington, A. Masic, N. Holten-Andersen, J. H. Waite and P. Fratzl, Science, 2010, 328, 216–220.
134 M. Krogsgaard, M. A. Behrens, J. S. Pedersen and H. Birkedal, Biomacromolecules, 2013, 14, 297–301.
135 J. V. Alegre-Requena, M. Häring, R. P. Herrera and D. D. Díaz, New J. Chem., 2016, 40, 8493–8501.
136 E. Filippidi, T. R. Cristiani, C. D. Eisenbach, J. H. Waite, J. N. Israelachvili, B. K. Ahn and M. T. Valentine, Science, 2017, 358, 502–505.
137 P. M. Lopez-Perez, R. M. P. da Silva, I. Strehin, P. H. J. Kouwer, S. C. G. Leeuwenburgh and P. B. Messersmith, Macromolecules, 2017, 50, 8698–8706.

138 H. Ceylan, M. Urel, T. S. Erkal, A. B. Tekinay, A. Dana and M. O. Guler, Adv. Funct. Mater., 2013, 23, 2081–2090.
139 Z. Li, Y. Shan, X. Wang, H. Li, K. Yang and Y. Cui, Chem. Eng. J., 2020, 124932.
140 W. Chen, Y. Bu, D. Li, Y. Liu, G. Chen, X. Wan and N. Li, J. Mater. Chem. C, 2020, 8, 900–908.
141 S. W. Taylor, G. W. Luther III and J. H. Waite, Inorg. Chem., 1994, 33, 5819–5824.
142 R. H. Holm, P. Kennepohl and E. I. Solomon, Chem. Rev., 1996, 96, 2239–2314.
143 N. Holten-Andersen, A. Jaishankar, M. J. Harrington, D. E. Fullenkamp, G. DiMarco, L. He, G. H. McKinley, P. B. Messersmith and K. Y. C. Lee, J. Mater. Chem. B, 2014, 2, 2467–2472.
144 A. Andersen, M. Krogsgaard and H. Birkedal, Biomacromolecules, 2017, 19, 1402–1409.
145 S. Hou and P. X. Ma, Chem. Mater., 2015, 27, 7627–7635.
146 R. M. Roat-Malone, Bioinorganic chemistry: a short course, John Wiley & Sons, 2007.
147 M. Kierstan and C. Bucke, Biotechnol. Bioeng., 2000, 67, 726.
148 P. Sikorski, F. Mo, G. Skjåk-Bræk and B. T. Stokke, Biomacromolecules, 2007, 8, 2098–2103.
149 M. Kierstan and C. Bucke, Biotechnol. Bioeng., 1977, 19, 387.
150 K. Zhang, Q. Feng, J. Xu, X. Xu, F. Tian, K. W. K. Yeung and L. Bian, Adv. Funct. Mater., 2017, 27, 1701642.
151 K. Zhang, W. Yuan, K. Wei, B. Yang, X. Chen, Z. Li, Z. Zhang and L. Bian, Small, 2019, 15, 1900242.
152 L. Shi, F. Wang, W. Zhu, Z. Xu, S. Fuchs, J. Hilborn, L. Zhu, Q. Ma, Y. Wang, X. Weng and D. A. Ossipov, Adv. Funct. Mater., 2017, 27, 1700591.
153 Q. Zhang, S. Niu, L. Wang, J. Lopez, S. Chen, Y. Cai, R. Du, Y. Liu, J.-C. Lai, L. Liu, C.-H. Li, X. Yan, C. Liu, J. B.-H. Tok, X. Jia and Z. Bao, Adv. Mater., 2018, 30, 1801435.
154 Y.-L. Rao, V. Feig, X. Gu, G.-J. Nathan Wang and Z. Bao, J. Polym. Sci., Part A: Polym. Chem., 2017, 55, 3110–3116.
155 D. Mozhdehi, J. A. Neal, S. C. Grindy, Y. Cordeau, S. Ayala, N. Holten-Andersen and Z. Guan, Macromolecules, 2016, 49, 6310–6321.
156 S. Bonnet, B. Limburg, J. D. Meeldijk, R. J. Klein Gebbink and J. A. Killian, J. Am. Chem. Soc., 2011, 133, 252–261.
157 C. Xie, W. Sun, H. Lu, A. Kretzschmann, J. Liu, M. Wagner, H.-J. Butt, X. Deng and S. Wu, Nat. Commun., 2018, 9, 3842.
158 J. Liu, C. Xie, A. Kretzschmann, K. Koynov, H.-J. Butt and S. Wu, Adv. Mater., 2020, 32, 1908324.
159 D. Yu, X. Zhao, C. Zhou, C. Zhang and S. Zhao, Macromol. Chem. Phys., 2017, 218, 1600519.
160 E. S. Epstein, L. Martinetti, R. H. Kollarigowda, O. Carey-De La Torre, J. S. Moore, R. H. Ewoldt and P. V. Braun, J. Am. Chem. Soc., 2019, 141, 3597–3604.
161 L. Zhang, Z. Liu, X. Wu, Q. Guan, S. Chen, L. Sun, Y. Guo, S. Wang, J. Song and E. M. Jeffries, Adv. Mater., 2019, 31, 1901402.
162 S. Götz, R. Geitner, M. Abend, M. Siegmann, S. Zechel, J. Vitz, S. Gräfe, M. Schmitt, J. Popp and M. D. Hager, Macromol. Rapid Commun., 2018, 39, 1800495.
163 J.-C. Lai, X.-Y. Jia, D.-P. Wang, Y.-B. Deng, P. Zheng, C.-H. Li, J.-L. Zuo and Z. Bao, Nat. Commun., 2019, 10, 1–9.
164 J.-C. Lai, L. Li, D.-P. Wang, M.-H. Zhang, S.-R. Mo, X. Wang, K.-Y. Zeng, C.-H. Li, Q. Jiang and X.-Z. You, Nat. Commun., 2018, 9, 1–9.
165 C.-H. Li, C. Wang, C. Keplinger, J.-L. Zuo, L. Jin, Y. Sun, P. Zheng, Y. Cao, F. Lissel, C. Linder, X.-Z. You and Z. Bao, Nat. Chem., 2016, 8, 618–624.
166 X.-Y. Jia, J.-F. Mei, J.-C. Lai, C.-H. Li and X.-Z. You, Macromol. Rapid Commun., 2016, 37, 952–956.
167 B. Sandmann, B. Happ, S. Kupfer, F. H. Schacher, M. D. Hager and U. S. Schubert, Macromol. Rapid Commun., 2015, 36, 604–609.
168 S. Bode, R. K. Bose, S. Matthes, M. Ehrhardt, A. Seifert, F. H. Schacher, R. M. Paulus, S. Stumpf, B. Sandmann, J. Vitz, A. Winter, S. Hoeppener, S. J. Garcia, S. Spange, S. van der Zwaag, M. D. Hager and U. S. Schubert, Polym. Chem., 2013, 4, 4966–4973.
169 M. Enke, L. Köps, S. Zechel, J. C. Brendel, J. Vitz, M. D. Hager and U. S. Schubert, Macromol. Rapid Commun., 2018, 39, 1700742.
170 J. Pignanelli, Z. Qian, X. Gu, M. J. Ahamed and S. Rondeau-Gagné, New J. Chem., 2020, 44, 8977–8985.
171 M. Enke, F. Jehle, S. Bode, J. Vitz, M. J. Harrington, M. D. Hager and U. S. Schubert, Macromol. Chem. Phys., 2017, 218, 1600458.
172 M. Chen, W. Wang, H. Chen, L. Bai, Z. Xue, D. Wei, H. Yang and Y. Niu, Macromol. Res., 2019, 27, 96–104.
173 D. Mozhdehi, S. Ayala, O. R. Cromwell and Z. Guan, J. Am. Chem. Soc., 2014, 136, 16128–16131.
174 Y. Kobayashi, T. Hirase, Y. Takashima, A. Harada and H. Yamaguchi, Polym. Chem., 2019, 10, 4519–4523.
175 J. P. Gong, Y. Katsuyama, T. Kurokawa and Y. Osada, Adv. Mater., 2003, 15, 1155–1158.
176 J. P. Gong, Soft Matter, 2010, 6, 2583–2590.
177 T. Nakajima, H. Sato, Y. Zhao, S. Kawahara, T. Kurokawa, K. Sugahara and J. P. Gong, Adv. Funct. Mater., 2012, 22, 4426–4432.
178 T. Nakajima, H. Furukawa, Y. Tanaka, T. Kurokawa, Y. Osada and J. P. Gong, Macromolecules, 2009, 42, 2184–2189.
179 E. Ducrot, Y. Chen, M. Bulters, R. P. Sijbesma and C. Creton, Science, 2014, 344, 186–189.
180 E. Ducrot and C. Creton, Adv. Funct. Mater., 2016, 26, 2482–2492.
181 T. Matsuda, T. Nakajima and J. P. Gong, Chem. Mater., 2019, 31, 3766–3776.
182 J.-Y. Sun, X. Zhao, W. R. K. Illeperuma, O. Chaudhuri, K. H. Oh, D. J. Mooney, J. J. Vlassak and Z. Suo, Nature, 2012, 489, 133–136.
183 C. Hu, M. X. Wang, L. Sun, J. H. Yang, M. Zrínyi and Y. M. Chen, Macromol. Rapid Commun., 2017, 38, 1600788.
184 X. He, C. Zhang, M. Wang, Y. Zhang, L. Liu and W. Yang, ACS Appl. Mater. Interfaces, 2017, 9, 11134–11143.
185 S. Hong, D. Sycks, H. F. Chan, S. Lin, G. P. Lopez, F. Guilak, K. W. Leong and X. Zhao, Adv. Mater., 2015, 27, 4035–4040.
186 M. X. Wang, C. H. Yang, Z. Q. Liu, J. Zhou, F. Xu, Z. Suo, J. H. Yang and Y. M. Chen, Macromol. Rapid Commun., 2015, 36, 465–471.

187 X.-H. Wang, F. Song, J. Xue, D. Qian, X.-L. Wang and Y.-Z. Wang, Polymer, 2018, 153, 637–642.
188 X. Li, H. Wang, D. Li, S. Long, G. Zhang and Z. Wu, ACS Appl. Mater. Interfaces, 2018, 10, 31198–31207.
189 G. Weng, Y. Huang, S. Thanneeru, H. Li, A. Alamri and J. He, Soft Matter, 2017, 13, 5028–5037.
190 X. Zhao, Soft Matter, 2014, 10, 672–687.
191 X.-H. Wang, F. Song, D. Qian, Y.-D. He, W.-C. Nie, X.-L. Wang and Y.-Z. Wang, Chem. Eng. J., 2018, 349, 588–594.
192 M. S. Menyo, C. J. Hawker and J. H. Waite, ACS Macro Lett., 2015, 4, 1200–1204.
193 C. Ma, Y. Wang, Z. Jiang, Z. Cao, H. Yu, G. Huang, Q. Wu, F. Ling, Z. Zhuang, H. Wang, J. Zheng and J. Wu, Chem. Eng. J., 2020, 399, 125697.
194 M. A. Gonzalez, J. R. Simon, A. Ghoorchian, Z. Scholl, S. Lin, M. Rubinstein, P. Marszalek, A. Chilkoti, G. P. López and X. Zhao, Adv. Mater., 2017, 29, 1604743.
195 Q. Chen, X. Yan, L. Zhu, H. Chen, B. Jiang, D. Wei, L. Huang, J. Yang, B. Liu and J. Zheng, Chem. Mater., 2016, 28, 5710–5720.
196 L. Zhang, Z. Liu, X. Wu, Q. Guan, S. Chen, L. Sun, Y. Guo, S. Wang, J. Song, E. M. Jeffries, C. He, F.-L. Qing, X. Bao and Z. You, Adv. Mater., 2019, 31, 1901402.
197 M. Yan, L. Cao, C. Xu and Y. Chen, Macromolecules, 2019, 52, 4329–4340.
198 M. H. Ghanian, H. Mirzadeh and H. Baharvand, Biomacromolecules, 2018, 19, 1646–1662.
199 G. Hong, H. Zhang, Y. Lin, Y. Chen, Y. Xu, W. Weng and H. Xia, Macromolecules, 2013, 46, 8649–8656.
200 Y. Chen, Z. Tang, Y. Liu, S. Wu and B. Guo, Macromolecules, 2019, 52, 3805–3812.
201 Z. Tang, J. Huang, B. Guo, L. Zhang and F. Liu, Macromolecules, 2016, 49, 1781–1789.
202 J. Huang, Z. Tang, Z. Yang and B. Guo, Macromol. Rapid Commun., 2016, 37, 1040–1045.
203 J. Liu, Z. Tang, J. Huang, B. Guo and G. Huang, Polymer, 2016, 97, 580–588.
204 M. Benaglia, A. Puglisi and F. Cozzi, Chem. Rev., 2003, 103, 3401–3430.
205 D. E. Bergbreiter, J. Tian and C. Hongfa, Chem. Rev., 2009, 109, 530–582.
206 D. E. Bergbreiter, ACS Macro Lett., 2014, 3, 260–265.
207 N. Madhavan, C. W. Jones and M. Weck, Acc. Chem. Res., 2008, 41, 1153–1165.
208 P. Bhyrappa, J. K. Young, J. S. Moore and K. S. Suslick, J. Am. Chem. Soc., 1996, 118, 5708–5711.
209 A. Ellis and L. J. Twyman, Macromolecules, 2013, 46, 7055–7074.
210 M. Zhao and R. M. Crooks, Angew. Chem., Int. Ed., 1999, 38, 364–366.
211 H. A. Zayas, A. Lu, D. Valade, F. Amir, Z. Jia, R. K. O'Reilly and M. J. Monteiro, ACS Macro Lett., 2013, 2, 327–331.
212 S. Wu, J. Dzubiella, J. Kaiser, M. Drechsler, X. Guo, M. Ballauff and Y. Lu, Angew. Chem., Int. Ed., 2012, 51, 2229–2233.
213 Y. Chen, Z. Wang, Y. W. Harn, S. Pan, Z. Li, S. Lin, J. Peng, G. Zhang and Z. Lin, Angew. Chem., Int. Ed., 2019, 58, 11910–11917.
214 D. E. Bergbreiter, V. M. Mariagnanam and L. Zhang, Adv. Mater., 1995, 7, 69–71.
215 W. Kramer and C. McCrory, Chem. Sci., 2016, 7, 2506–2515.
216 S. Thanneeru, J. K. Nganga, A. S. Amin, B. Liu, L. Jin, A. M. Angeles-Boza and J. He, ChemCatChem, 2017, 9, 1157–1162.
217 W. P. Brezinski, M. Karayilan, K. E. Clary, K. C. McCleary-Petersen, L. Fu, K. Matyjaszewski, D. H. Evans, D. L. Lichtenberger, R. S. Glass and J. Pyun, ACS Macro Lett., 2018, 7, 1383–1387.
218 S. Thanneeru, N. Milazzo, A. Lopes, Z. Wei, A. M. Angeles-Boza and J. He, J. Am. Chem. Soc., 2019, 141, 4252–4256.
219 C. S. McKay and M. G. Finn, Angew. Chem., Int. Ed., 2016, 55, 12643–12649.
220 J. A. Trindell, J. Clausmeyer and R. M. Crooks, J. Am. Chem. Soc., 2017, 139, 16161–16167.
221 L. Zhang, Z. Wei, S. Thanneeru, M. Meng, M. Kruzyk, G. Ung, B. Liu and J. He, Angew. Chem., Int. Ed., 2019, 131, 15981–15987.
222 G. E. Oosterom, J. N. H. Reek, P. C. J. Kamer and P. W. N. M. van Leeuwen, Angew. Chem., Int. Ed., 2001, 40, 1828–1849.
223 J. W. J. Knapen, A. W. van der Made, J. C. de Wilde, P. W. N. M. van Leeuwen, P. Wijkens, D. M. Grove and G. van Koten, Nature, 1994, 372, 659–663.
224 A. Ouali, R. Laurent, A.-M. Caminade, J.-P. Majoral and M. Taillefer, J. Am. Chem. Soc., 2006, 128, 15990–15991.
225 C. S. McKay and M. Finn, Angew. Chem., Int. Ed., 2016, 128, 12833–12839.
226 T. Yamamoto, T. Yamada, Y. Nagata and M. Suginome, J. Am. Chem. Soc., 2010, 132, 7899–7901.
227 J. P. Leonard, M. Fabrizio and S. Paolo, Curr. Org. Chem., 2009, 13, 1050–1064.
228 W. P. Brezinski, M. Karayilan, K. E. Clary, N. G. Pavlopoulos, S. Li, L. Fu, K. Matyjaszewski, D. H. Evans, R. S. Glass, D. L. Lichtenberger and J. Pyun, Angew. Chem., Int. Ed., 2018, 57, 11898–11902.
229 Y. Liu and C. C. McCrory, Nat. Commun., 2019, 10, 1–10.
230 F. Wang, W. J. Liang, J. X. Jian, C. B. Li, B. Chen, C. H. Tung and L. Z. Wu, Angew. Chem., Int. Ed., 2013, 125, 8292–8296.
231 T. Yu, Y. Zeng, J. Chen, Y. Y. Li, G. Yang and Y. Li, Angew. Chem., Int. Ed., 2013, 52, 5631–5635.
232 E. Verde-Sesto, A. Arbe, A. Moreno, D. Cangialosi, Á. Alegría, J. Colmenero and J. A. Pomposo, Mater. Horiz., 2020, 7, 2292–2313.
233 J. Rubio-Cervilla, E. González and J. A. Pomposo, Nanomaterials, 2017, 7, 341.
234 O. Altintas and C. Barner-Kowollik, Macromol. Rapid Commun., 2012, 33, 958–971.
235 A. Latorre-Sánchez and J. A. Pomposo, Polym. Int., 2016, 65, 855–860.
236 H. Rothfuss, N. D. Knöfel, P. W. Roesky and C. Barner-Kowollik, J. Am. Chem. Soc., 2018, 140, 5875–5881.
237 A. Sanchez-Sanchez, A. Arbe, J. Colmenero and J. A. Pomposo, ACS Macro Lett., 2014, 3, 439–443.
238 A. Sanchez-Sanchez, A. Arbe, J. Kohlbrecher, J. Colmenero and J. A. Pomposo, Macromol. Rapid Commun., 2015, 36, 1592–1597.

239 Y. Bai, X. Feng, H. Xing, Y. Xu, B. K. Kim, N. Baig, T. Zhou, A. A. Gewirth, Y. Lu, E. Oldfield and S. C. Zimmerman, J. Am. Chem. Soc., 2016, 138, 11077–11080.
240 R. Lambert, A.-L. Wirotius, S. Garmendia, P. Berto, J. Vignolle and D. Taton, Polym. Chem., 2018, 9, 3199–3204.
241 M. Artar, E. R. J. Souren, T. Terashima, E. W. Meijer and A. R. A. Palmans, ACS Macro Lett., 2015, 4, 1099–1103.
242 N. D. Knöfel, H. Rothfuss, J. Willenbacher, C. Barner-Kowollik and P. W. Roesky, Angew. Chem., Int. Ed., 2017, 56, 4950–4954.
243 J. Willenbacher, O. Altintas, V. Trouillet, N. Knöfel, M. J. Monteiro, P. W. Roesky and C. Barner-Kowollik, Polym. Chem., 2015, 6, 4358–4365.
244 M. Artar, T. Terashima, M. Sawamoto, E. Meijer and A. R. Palmans, J. Polym. Sci., Part A: Polym. Chem., 2014, 52, 12–20.
245 A. Levy, R. Feinstein and C. E. Diesendruck, J. Am. Chem. Soc., 2019, 141, 7256–7260.
246 S. Mavila, I. Rozenberg and N. G. Lemcoff, Chem. Sci., 2014, 5, 4196–4203.
247 Y. Zhang, R. Tan, M. Gao, P. Hao and D. Yin, Green Chem., 2017, 19, 1182–1193.
248 N. D. Knöfel, H. Rothfuss, J. Willenbacher, C. Barner-Kowollik and P. W. Roesky, Angew. Chem., Int. Ed., 2017, 56, 4950–4954.
249 Y. Zhang, W. Wang, W. Fu, M. Zhang, Z. Tang, R. Tan and D. Yin, Chem. Commun., 2018, 54, 9430–9433.
250 S. Mavila, I. Rozenberg and N. G. Lemcoff, Chem. Sci., 2014, 5, 4196–4203.
251 S. Mavila, C. E. Diesendruck, S. Linde, L. Amir, R. Shikler and N. G. Lemcoff, Angew. Chem., Int. Ed., 2013, 125, 5879–5882.
252 T. Terashima, A. Nomura, M. Ito, M. Ouchi and M. Sawamoto, Angew. Chem., Int. Ed., 2011, 50, 7892–7895.
253 T. Terashima, M. Ouchi, T. Ando and M. Sawamoto, Polym. J., 2011, 43, 770–777.
254 C. Kulkarni, E. Meijer and A. R. Palmans, Acc. Chem. Res., 2017, 50, 1928–1936.
255 T. Terashima, T. Mes, T. F. A. De Greef, M. A. J. Gillissen, P. Besenius, A. R. A. Palmans and E. W. Meijer, J. Am. Chem. Soc., 2011, 133, 4742–4745.
256 T. Mes, R. van der Weegen, A. R. A. Palmans and E. W. Meijer, Angew. Chem., Int. Ed., 2011, 50, 5085–5089.
257 N. Hosono, A. R. A. Palmans and E. W. Meijer, Chem. Commun., 2014, 50, 7990–7993.
258 M. A. J. Gillissen, I. K. Voets, E. W. Meijer and A. R. A. Palmans, Polym. Chem., 2012, 3, 3166–3174.
259 N. Hosono, A. M. Kushner, J. Chung, A. R. A. Palmans, Z. Guan and E. W. Meijer, J. Am. Chem. Soc., 2015, 137, 6880–6888.
260 P. J. M. Stals, C.-Y. Cheng, L. van Beek, A. C. Wauters, A. R. A. Palmans, S. Han and E. W. Meijer, Chem. Sci., 2016, 7, 2011–2015.
261 P. J. M. Stals, M. A. J. Gillissen, T. F. E. Paffen, T. F. A. de Greef, P. Lindner, E. W. Meijer, A. R. A. Palmans and I. K. Voets, Macromolecules, 2014, 47, 2947–2954.
262 G. M. ter Huurne, M. A. J. Gillissen, A. R. A. Palmans, I. K. Voets and E. W. Meijer, Macromolecules, 2015, 48, 3949–3956.
263 E. Huerta, B. van Genabeek, P. J. M. Stals, E. W. Meijer and A. R. A. Palmans, Macromol. Rapid Commun., 2014, 35, 1320–1325.
264 M. A. J. Gillissen, T. Terashima, E. W. Meijer, A. R. A. Palmans and I. K. Voets, Macromolecules, 2013, 46, 4120–4125.
265 E. Huerta, P. J. Stals, E. Meijer and A. R. Palmans, Angew. Chem., Int. Ed., 2013, 125, 2978–2982.
266 Y. Liu, S. Pujals, P. J. Stals, T. Paulöhrl, S. I. Presolski, E. Meijer, L. Albertazzi and A. R. Palmans, J. Am. Chem. Soc., 2018, 140, 3423–3433.
267 L. Wang, B. Song, Y. Li, L. Gong, X. Jiang, M. Wang, S. Lu, X.-Q. Hao, Z. Xia, Y. Zhang, S. W. Hla and X. Li, J. Am. Chem. Soc., 2020, 142, 9809–9817.
268 J. Liu, C. Xie, A. Kretzschmann, K. Koynov, H. J. Butt and S. Wu, Adv. Mater., 2020, 32, 1908324.
269 Y. Gu, E. A. Alt, H. Wang, X. Li, A. P. Willard and J. A. Johnson, Nature, 2018, 560, 65–69.

